



**KTH Architecture and
the Built Environment**

Characterising the Deformation Behaviour of Unbound Granular Materials in Pavement Structures

Mohammad Shafiqur Rahman

Doctoral Thesis

Division of Highway and Railway Engineering
Department of Civil and Architectural Engineering
KTH Royal Institute of Technology
SE-100 44 Stockholm
Sweden 2015

© Mohammad Shafiqur Rahman

Stockholm 2015

TRITA-TSC-PHD 15-004

ISBN 978-91-87353-68-0

CONTENTS

Preface	iii
Abstract	v
List of Appended Papers	vii
Other Relevant Papers	ix
List of Symbols	xi
List of Acronyms	xv
List of Figures	xvii
List of Tables	xxi
1. Introduction	1
1.1 General overview	1
1.2 Objectives and methodology.....	3
2. In Situ Pavement Conditions	5
2.1 Stresses	5
2.2 Moisture.....	8
3. Deformation Behaviour of UGMs	11
3.1 RD characteristics.....	12
3.1.1 Modelling the RD behaviour with respect to stresses	12
3.1.2 Influence of moisture on M_R	12
3.2 PD characteristics	14
3.2.1 Modelling the PD behaviour with respect to stresses.....	17
3.2.2 Influence of moisture on PD	19
4. Experimental Study	21
4.1 The RLT test	21
4.2 Description of the equipment	22
4.3 Specimen preparation	24
4.4 Test procedure.....	26
4.5 Materials used and tests performed	30
4.6 Some considerations regarding the test procedure.....	34
5. Results and Analyses	37
5.1 Calculations.....	37

5.2 Calibration of the models	37
5.3 Statistical evaluation of the quality of fit	37
5.4 Shakedown range calculation	38
6. Summary of the Appended Papers.....	41
6.1 Paper I: Moisture Influence on the RD Behaviour of UGMs.....	41
6.2 Paper II: Evaluation of PD Characteristics of UGMs by Means of MS RLT tests .	49
6.3 Paper III: Predicting PD Behaviour of UGMs.....	53
6.4 Paper IV: Characterizing the Impact of Moisture on the PD Behaviour of UGMs .	58
6.5 Paper V: A Model for Predicting PD of UGMs	60
7. Conclusions	65
7.1 Major findings	65
7.2 Some limitations	66
7.3 Recommendations for future work	67
References.....	69

PREFACE

This Ph.D. project was carried out at the Swedish National Road and Transport Research Institute (VTI) in co-operation with the KTH Royal Institute of Technology. It was financed by the Swedish Transport Administration (Trafikverket). The Danish aggregates used here were provided by the Danish Road Directorate. This work was supervised by Professor Sigurdur Erlingsson at VTI.

First, I would like to express my gratitude to VTI for allowing me the opportunity to work on this project. I am very grateful to my supervisor Professor Sigurdur Erlingsson for all his guidance, support, inputs, insightful ideas, constructive comments, patience and very warm and friendly attitude.

I am also thankful to our former head of the Department of Pavement Technology at VTI, Gunilla Franzén, and the current head of the department, Björn Kalman, for administrative support. My special thanks go to Håkan Arvidsson for helping me in the laboratory.

I am also indebted to my fellow Ph.D. students at VTI, Abubeker Ahmed, Farhad Salour, Jonas Wennström and Markus Svensson, who have always helped and inspired me in many ways. I am also thankful to my colleagues for the friendly environment and for their help and support directly and indirectly all through the project. I would like to specifically mention Hassan Hakim for his help and invaluable suggestions in many different aspects.

Finally, I am grateful to my wife Nadia Sharmin and my daughters Farishta and Aura for all their love and support. I am also thankful to my parents and siblings for their inspiration.

Mohammad Shafiqur Rahman

Linköping, March 2015

ABSTRACT

Unbound granular materials (UGMs) used in the base and sub-base layers of flexible pavements play a significant role in the overall performance of the structure. Proper understanding and characterization of the deformation behaviour of UGMs in pavement structures are, therefore, vital for the design and maintenance of flexible pavements. In this study, the resilient deformation (RD) and the permanent deformation (PD) behaviour of UGMs were investigated for the better understanding and improved modelling of these deformation characteristics. The study is based on a series of repeated-load triaxial (RLT) tests carried out on several UGMs commonly used in pavement structures. Here, the influences of stress level and moisture content - two of the most significant factors affecting the deformation behaviour of UGMs - were analysed. The effects of the grain size distribution and the degree of compaction were also considered.

The study on the RD behaviour indicated that the resilient stiffness (M_R) of UGMs increases with the increased bulk stress level, which can be satisfactorily described by the k - θ model. Moisture was found to negatively impact the M_R as long as the deformation was mostly resilient with a negligible amount of accumulated PD. Analysis of the influence of moisture on the parameters k_1 and k_2 of the k - θ model showed that k_1 decreases with increased moisture and k_2 is relatively insensitive to moisture. Based on these observations, a simple model was developed for the impact of moisture on M_R . The performance of this model was comparable to an existing moisture dependent M_R model. In contrast, it was further observed that at the later stages of the RLT tests, after a relatively large number of load applications, the M_R increased with increased moisture up to the optimum moisture content. This occurred when the RD was accompanied by a significant amount of PD. Further investigation suggested that moisture aided the post-compaction (PC) and possible particle rearrangement that resulted in the increased PD and increased M_R . In this case k_1 decreased, whereas k_2 increased, with increased moisture. The existing M_R -moisture model did not work for this behaviour. This suggests that the effect of PC on M_R should be considered in modelling. However, although not explored in this study, it may be possible to simulate this effect of increase in M_R with increased moisture due to PC using the proposed model if k_2 is expressed as a function of moisture.

The PD characteristics of UGMs were investigated based on the multistage (MS) RLT test. In contrast with the single stage (SS) RLT test, the MS RLT test accounts for the effect of stress history and enables a comprehensive study of the material behaviour under cyclic stresses of various magnitudes. Since the existing PD models cannot be directly applied for the MS loading procedure, a general formulation based on the time hardening concept was derived that can be used to extend the models for the MS loading conditions. Based on this formulation, some of the current models were calibrated and their performance in predicting the PD behaviour in MS RLT tests was compared. The investigation regarding

the impact of moisture on PD showed that moisture significantly increases the accumulation of PD. Generally, materials with finer grading showed more sensitivity to moisture with regards to both PD and RD. To characterize the impact of moisture, moisture sensitivity of different grain size distributions and the impact of the degree of compaction on PD with reduced effort, a simple model was proposed. Unlike some of the well-performing existing models, this model can be calibrated using a single MS RLT test without requiring any separate static failure triaxial tests. This model was validated using the MS RLT test data with satisfactory results. The sensitivity of the parameters of this model was studied with respect to moisture content, degree of compaction and grain size distribution. Some reasonable trends for the sensitivity of the parameters to these influential factors were obtained, which suggests that these may be further developed to incorporate into the model.

Keywords: unbound granular materials, resilient modulus, permanent deformation, moisture, model, multistage, repeated-load triaxial test.

LIST OF APPENDED PAPERS

This doctoral thesis is based on the following five interrelated papers, enclosed at the end. These are referred to in the text by the Roman numerals:

- I. Rahman, M.S. and Erlingsson, S. (2015). Moisture Influence on the Resilient Deformation Behaviour of Unbound Granular Materials. *International Journal of Pavement Engineering*, in press. DOI: 10.1080/10298436.2015.1019497.
- II. Erlingsson, S. and Rahman, M.S. (2013). Evaluation of Permanent Deformation Characteristics of Unbound Granular Materials by Means of Multistage Repeated-Load Triaxial Tests. *Transportation Research Record: Journal of the Transportation Research Board*, Transportation Research Board of the National Academies, Washington, D.C., No. 2369, 11-19. DOI: 10.3141/2369-02.
- III. Rahman, S. and Erlingsson, S. (2014). Predicting Permanent Deformation Behaviour of Unbound Granular Materials. *International Journal of Pavement Engineering*, DOI: 10.1080/10298436.2014.943209.
- IV. Rahman, M.S. and Erlingsson, S. (2015). Characterizing the Impact of Moisture on the Permanent Deformation Behaviour of Unbound Granular Materials. *Compendium of Papers of the 94th Annual Meeting of the Transportation Research Board*, Washington DC.
- V. Rahman, M.S. and Erlingsson, S. (2015). A Model for Predicting Permanent Deformation of Unbound Granular Materials. *Road Materials and Pavement Design*, in press. DOI: 10.1080/14680629.2015.1026382.

OTHER RELEVANT PAPERS

- I. Rahman, S. and Erlingsson, S. (2012). Moisture Sensitivity of Unbound Granular Materials. *Proceedings of the 4th European Pavement and Asset Management Conference (EPAM4)*, September, 2012, Malmö, Sweden.
- II. Rahman, M.S. and Erlingsson, S. (2013). Moisture Sensitivity of the Deformation Properties of Unbound Granular Materials. *Proceedings of the 9th International Conference on Bearing Capacity of Roads and Airfields, BCRRA '13*, Trondheim, Norway, pp. 777-786.
- III. Rahman, M.S. and Erlingsson, S. (2014). Influence of Moisture on the Resilient Deformation Behaviour of Unbound Granular Materials. In Y.R. Kim (Ed.) *Asphalt Pavements - Proceedings of the International Conference on Asphalt Pavements (ISAP)*, Raleigh, North Carolina, 1 – 5 June, pp. 571 - 580. CRC Press – Taylor and Francis Group, ISBN 978-1-138-02693-3.
- IV. Erlingsson, S. and Rahman, M.S. (2013). Evaluation of Permanent Deformation Characteristics of Unbound Granular Materials using Multi-stage Repeated-Load Triaxial Tests. *Compendium of Papers of the Annual Meeting of the Transportation Research Board*, Transportation Research Board of the National Academies, Washington DC.
- V. Rahman, M.S. and Erlingsson, S. (2014). Permanent Deformation Models of Unbound Granular Materials: A Comparative Study Based on Multi-Stage Repeated-Load Triaxial Tests. *Compendium of Papers of the Annual Meeting of the Transportation Research Board*, Transportation Research Board of the National Academies, Washington DC.

LIST OF SYMBOLS

a	the minimum of $\log (M_R/M_{Ropt})$
a	material parameter of the proposed permanent deformation model (Equation 26)
a_1	material parameter of the proposed M_R -moisture model (Equation 14)
a_2	material parameter of the proposed M_R -moisture model (Equation 14)
A	parameter of the Korkiala-Tanttu model usually taken as 1.05
b	the maximum of $\log (M_R/M_{Ropt})$
b	material parameter of the Korkiala-Tanttu model
b	material parameter of the proposed permanent deformation model (Equation 26)
B	material parameter of the Gidel et al. model
C	material parameter of the Korkiala-Tanttu model
c	material parameter of the modified Korkiala-Tanttu model
c_1	parameter of the equation for the variation of the parameter a of the proposed permanent deformation model as a function of moisture content
c_2	parameter of the equation for the variation of the parameter a of the proposed permanent deformation model as a function of moisture content
d	material parameter of the modified Korkiala-Tanttu model
D	size of the sieve opening
D_{max}	the maximum particle size
G_s	specific gravity of the particles of a UGM
f_i	a predicted value by a model

i	stress path number
k_1, k_2	material parameters of the k - θ model
k_m	material parameter of the MEPDG M_R -Moisture model
L_{\max}	a parameter of the Gidel et al. model expressed as $L_{\max} = \sqrt{p_{\max}^2 + q_{\max}^2}$
m	the slope of the Mohr-Coulomb failure line in p - q space
M_R	resilient modulus
M_{Ropt}	resilient modulus at optimum moisture content
n	the grading coefficient
n	material parameter of the Gidel et al. model (replaced by u in paper III)
N	the number of load cycles
n_d	the number of data points
N_i	the total number of load cycles at the end of i^{th} stress path
N_i^{eq}	the equivalent number of load cycles
p	hydrostatic stress
P	the percentage of particles smaller than sieve size D in Fuller's equation
p_a	reference pressure (100 kPa)
p_m	the number of regression parameters in a model
p_{\max}	the maximum applied hydrostatic stress
q	cyclic deviator stress
q_f	the deviator stress at failure
q_{\max}	the maximum applied deviator stress

R	is a ratio of the applied deviator stress to the deviator stress at failure, determined using static failure triaxial tests
$RMSE$	root mean square error
R^2	the coefficient of determination
s	the intercept of the Mohr-Coulomb failure line in p - q space
S	the degree of saturation
S	in Paper IV, S is the same entity as S_f
S_f	the term describing the effect of stress condition on the development of permanent deformation in the proposed model (Equation 26)
S_{opt}	Degree of saturation at w_{opt}
SS_{res}	the residual sum of squares
SS_{tot}	the total sum of squares
u	material parameter of the Gidel et al. model
w	gravimetric moisture content
W_c	gravimetric moisture content (in papers II and III)
w_{opt}	gravimetric optimum moisture content
y_i	a measured data point
\bar{y}	the mean of the measured data
α	material parameter of the proposed permanent deformation model (Equation 26)
β	material parameter of the Tseng and Lytton model
γ_w	dry unit weight of water
γ_{dry}	dry density of a test specimen

ε_0	material parameter of the Tseng and Lytton model
ε^0	material parameter of the Gidel et al. model
ε_p	axial permanent strain
ε_r	axial resilient strain
ε_{tot}	total axial strain
$\hat{\varepsilon}_p$	the accumulated permanent strain
$\hat{\varepsilon}_p(N)$	the accumulated permanent strain after N number of load cycles
$\hat{\varepsilon}_p^{3000}$	accumulated permanent strain at 3000 th load cycles in the RLT test
$\hat{\varepsilon}_p^{5000}$	accumulated permanent strain at 5000 th load cycles in the RLT test
$\hat{\varepsilon}_{p_i}$	the accumulated permanent strain at the end of i^{th} stress path
$\hat{\varepsilon}_{p_i}'$	the apparent accumulated permanent strain at the end of i^{th} stress path
θ	sum of the principal stresses (bulk stress)
ρ	material parameter of the Tseng and Lytton model
$\sigma_1, \sigma_2, \sigma_3$	principal stresses
σ_c	confining pressure
σ_d	cyclic deviator stress
σ_{dmin}	the minimum deviator stress during cyclic loading

LIST OF ACRONYMS

AASHTO	-	American Association of State Highway and Transportation Officials
AC	-	Asphalt Concrete
APT	-	Accelerated Pavement Tests
FE	-	Finite Element
FWD	-	Falling Weight Deflectometer
HSL	-	High Stress Level
HVS	-	Heavy Vehicle Simulator
LDT	-	Local Deformation Transducer
LSL	-	Low Stress Level
LVDT	-	Linear Variable Displacement Transducer
ME	-	Mechanistic-Empirical
MEPDG	-	Mechanistic Empirical Pavement Design Guide
MS	-	Multistage
PC	-	Post Compaction
PD	-	Permanent Deformation
RD	-	Resilient Deformation
RLT	-	Repeated-load Triaxial
SS	-	Single Stage
UGM	-	Unbound Granular Material
VBA	-	Visual Basic for Applications

LIST OF FIGURES

Figure 1. (a) Rutting, (b) fatigue cracking.	1
Figure 2. Mechanistic-Empirical design approach.	2
Figure 3. Stresses in UGMs due to moving wheel load (Lekarp 1999).	6
Figure 4. Lateral wander of traffic on a typical Swedish arterial road (Erlingsson et al. 2012)	6
Figure 5. The pavement structure IS02, used for the HVS tests and FE analyses (Erlingsson 2002).	7
Figure 6. Comparison of measurements and FE analyses for IS 02 single wheel configuration, profile 1. The wheel load was in all cases 60 kN, whereas the tyre pressures were 500 kPa, 600 kPa, 800 kPa and 900 kPa, respectively (Erlingsson 2002).	7
Figure 7. An illustration of moisture balance in a pavement structure (Erlingsson et al. 2009).	8
Figure 8. A typical variation in moisture content in the granular base and subgrade of a low traffic pavement (near the pavement edge) (Charlier et al. 2009).	9
Figure 9. Strains in UGMs under cyclic loading.	11
Figure 10. Variation in stiffness (back-calculated based on FWD measurements) with the variation of volumetric moisture content in a typical granular sub-base layer (Salour and Erlingsson 2013).	13
Figure 11. Development of rutting due to PD of the UGMs.	14
Figure 12. Development of PD at constant versus multiple stress levels.	15
Figure 13. Different types of PD behaviour, depending on stress level (Dawson and Wellner 1999, Werkmeister et al. 2001).	16
Figure 14. Effect of stress history in modelling the accumulation of PD in MS RLT tests.	19
Figure 15. Effect of moisture on the accumulation of PD in an HVS test section. The vertical line indicates the introduction of water (Saevarsdottir and Erlingsson 2013).	20
Figure 16. Principles of the RLT test (Erlingsson and Magnúsdóttir 2002).	21

Figure 17. (a) Schematic overview of the triaxial test cell, (b) axial LVDTs mounted on the specimen, (c) triaxial cell placed in the loading frame.	23
Figure 18. (a) The studs that are placed inside the specimen, (b) the LVDT holders, (c) the studs mounted inside the cylindrical mould before preparation of the specimen.	23
Figure 19. Schematic of the servo-hydraulic RLT test system.	24
Figure 20. Specimen preparation: (a) vibrocompaction, (b) hydraulic extraction (Arvidsson 2006).	25
Figure 21. (a) Stress state in the triaxial cell, (b) stress paths for HSL, (c) stress paths for LSL.	28
Figure 22. A typical registration of six load pulses and corresponding deformations.	29
Figure 23. Typical stress versus strain plots for a few cycles of loading in a PD test ($\sigma_d = 280$ kPa, $\sigma_3 = 70$ kPa).	29
Figure 24. Pictures of the UGMs tested: (a) Skärlunda, (b) Hallinden, (c) SPV, (d) VKB, (e) Siem, (f) SG1.	30
Figure 25. Grain size distribution curves of the UGMs tested.	31
Figure 26. M_R as a function of θ for various w and S from the RD tests: (a) Skärlunda ($n = 0.35$), (b) SG1.	42
Figure 27. The parameters k_1 and k_2 as a function of S from the RD tests.	43
Figure 28. Normalized M_R as a function of change in S (for $\theta = 550$ kPa): Modelled vs. measured.	44
Figure 29. M_R as a function of θ for various w and S from the PD tests: (a) Skärlunda ($n = 0.35$) (b) SG1.	45
Figure 30. The parameters k_1 and k_2 as a function of S from the PD tests.	46
Figure 31. Evolution of M_R with N and PD for different shakedown ranges (for Skärlunda ($n = 0.35$), $w = 2\%$ and 3.5% , PD test with HSL).	47
Figure 32. Comparison of the M_R values from the RD test and the PD tests with the HSL and the LSL for Skärlunda ($n = 0.35$) with $w = 2\%$	48
Figure 33. Demonstration of the time hardening approach.	49
Figure 34. Accumulation of permanent strain: Test data and the calibrated models.	52

Figure 35. Accumulation of permanent strain: Test data and the calibrated models: (a) for the calibration test and (b) for the validation test.	54
Figure 36. Accumulated permanent strain: Predicted versus measured plots (a) for the calibration test and (b) for the validation test.	55
Figure 37. Comparison of the quality of fit (adjusted R^2 values).	56
Figure 38. Accuracy of the shakedown range predictions [%].	56
Figure 39. Measured and modelled accumulation of permanent strain for a series of w for the different grain size distributions of the Skärlanda UGMs.	59
Figure 40. Measured and modelled accumulation of permanent strain for a series of w for different UGMs (during calibration).	60
Figure 41. Parameter a as a function of moisture content for the different materials.	62
Figure 42. Parameter a as a function of the degree of compaction.	63
Figure 43. Predicted accumulation of permanent strain using the calibrated models in different stress conditions against the measured values.	64

LIST OF TABLES

Table 1. Stress levels used for the resilient modulus tests (CEN 2004a).....	26
Table 2. Stress levels used for the PD tests (HSL) (CEN 2004a).	27
Table 3. Stress levels used for the PD tests (LSL) (CEN 2004a).....	27
Table 4. List of the RD (RLT) tests performed.	32
Table 5. List of the PD (RLT) tests performed.	32
Table 6. List of the static failure triaxial tests performed.	33
Table 7. An example of the shakedown range predictions by the models (Siem 30, $w = 3.5\%$, LSL).	39
Table 8. Calibrated material parameters of the model.	61
Table 9. Parameters of Equation (30).	62

1. INTRODUCTION

1.1 General overview

Flexible pavements are layered structures where the stiffer asphalt concrete (AC) top layer(s) are placed above the base and sub-base layers. The base and sub-base layers are usually composed of unbound (no binder is used) granular materials (UGMs). The UGMs are generally aggregates of different sizes and shapes, most commonly originating from natural gravel or crushed rock or a mixture of both. The base and sub-base layers provide the structural support for the AC layers and contribute to the load spreading mechanism of the system. The mechanical properties and deformation behaviour of the UGMs are, therefore, very important for the stability and performance of the pavement structure.

The principal function of pavements is to provide a smooth and safe riding surface by reducing stresses in the subgrade to a tolerable limit. However, the functionality of pavements deteriorates with time due to the traffic loading and climatic conditions. Two of the major distress modes of pavements are rutting and fatigue cracking, shown in Figure 1. Rutting is the channelized depression along the wheel path and fatigue cracking is characterized as a series of longitudinal and interconnected cracks on the surface of the pavement.



(a)

(b)

Figure 1. (a) Rutting, (b) fatigue cracking.

The objective of pavement design is to come up with an optimum combination of materials and layer-thicknesses based on strength, durability, availability, field conditions and economic considerations which can withstand the traffic loading and the environmental conditions for the design life of the pavement with minimum distresses. This is usually done employing empirical methods. However, empirical methods cannot provide satisfactory results in many instances. Because of this, there has been a growing interest in developing a mechanistic-empirical (ME) design approach. A schematic of the ME design approach has been shown in Figure 2. The basis for this approach is the prediction of the

performance of the constituent materials in the pavement structure through characterization of their mechanical behaviour as realistically as possible. This is also required for the maintenance and rehabilitation projects and for the life-cycle cost analysis of pavements. In the ME design process, the performance prediction of the constituent materials is done with the use of constitutive models. Developing such models requires extensive laboratory and field testing and analysis of the generated data. Ideally, the constitutive models should be able to reliably predict the deformation behaviour of the materials considering the major influencing factors on the behaviour. However, because of the complexity of the tests, nonlinear and complex constitutive relations of the materials, and difficulties in correlating laboratory test results to in-pavement behaviour (Uzan 2004, Hornych and El Abd 2004, Gidel et al. 2001), development of such models is still underway.

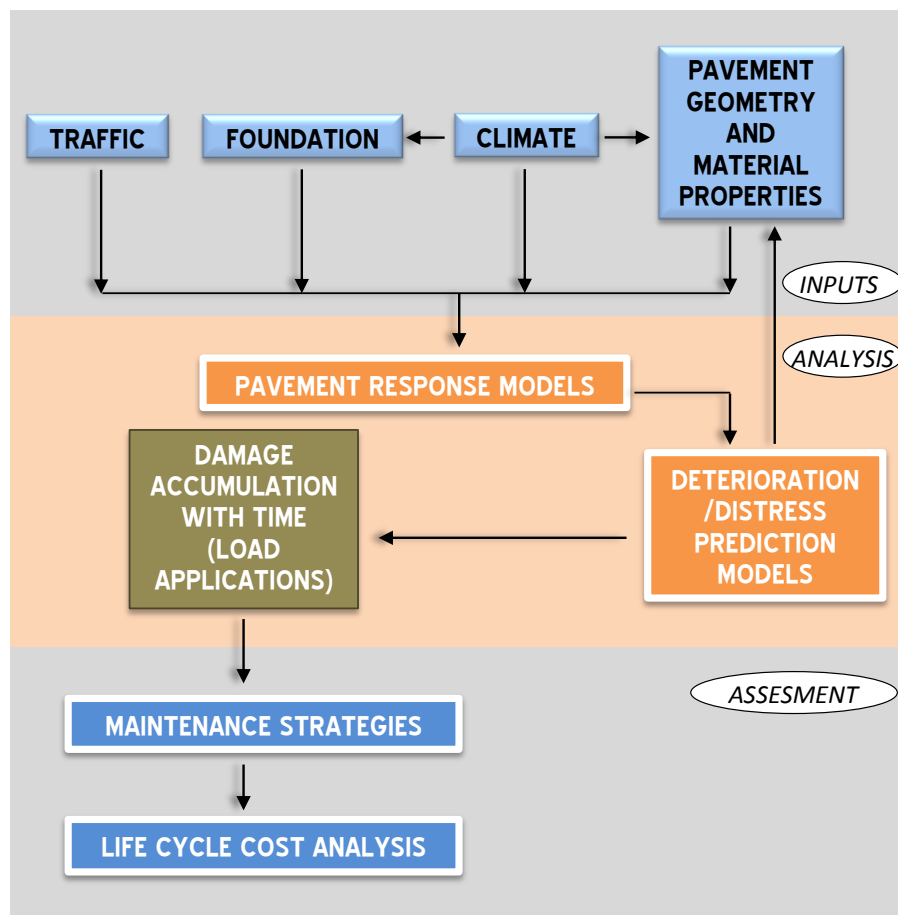


Figure 2. Mechanistic-Empirical design approach.

This thesis deals with the deformation behaviour UGMs. The focus of this study was the external factors that have the most significant influence on the mechanical properties of UGMs in pavements: (a) stresses from the traffic loading and (b) moisture variation due to climatic conditions. This thesis is based on three published papers and two submitted manuscripts that are appended at the end. The following sections present the specific objectives, brief reviews of some relevant background, the test procedure and summaries of the papers with some supplementary information.

1.2 Objectives and methodology

The general objective of this work was to enhance the understanding and to improve the modelling of the deformation behaviour of UGMs. With this aim, repeated-load triaxial (RLT) tests were performed on some UGMs typically used in the base layers of flexible pavements. For a realistic approach, the multistage (MS) loading procedure was preferred. To investigate the major influencing factors on the deformation behaviour, the RLT tests were performed applying a range of stress levels on specimens having different grain size distributions, with a series of moisture contents and at a few different degrees of compaction. Specifically the scope of the work was:

- To study the influence of moisture on the resilient deformation (RD) properties of UGMs. Especially, to differentiate the nature of the moisture impact when the deformation is mostly resilient and when the RD is accompanied by significant amount of accumulated permanent deformation (PD). The sensitivity to moisture for different grain size distributions was also given consideration. The performance of an existing moisture dependent resilient modulus (M_R) model was investigated, as was the variation of the parameters of the k - θ model with moisture. Based on this an alternative modelling approach for the impact of moisture on the M_R was explored. These have been accomplished in Paper I.
- To formulate an approach to use the existing PD models for MS loading conditions for better and more comprehensive characterization of the PD behaviour of UGMs. This has been accomplished in Paper II.
- To implement some of the existing PD models for MS loading conditions using the formulation introduced in Paper II and to validate and compare their performance. This was done in Paper III.
- To characterize the impact of moisture on the PD behaviour of UGMs. To reduce the effort generally required for the existing PD models, a simple model was developed containing relatively fewer material parameters that can be evaluated using a single MS RLT test without the need for the additional static failure triaxial tests. The sensitivity of the parameters of this model was studied with respect to moisture content, degrees of compaction and grain size distribution with the aim of incorporating these into the model in future. These were attempted in Paper IV and Paper V.

In this study only the axial deformation was considered. The moisture contents reported here refer to the gravimetric moisture content expressed as a percentage.

2. IN SITU PAVEMENT CONDITIONS

Pavement structures in the field are subjected to various forms of traffic loading and a wide range of environmental and climatic conditions. Traffic loading can vary a great deal depending on the classification and location of the road. Severity of the environmental conditions mostly depends on the geographical location. The two most significant climatic factors for pavements are probably temperature and moisture. The behaviour of UGMs in the base and sub-base layers of pavements is mostly affected by stresses due to traffic loading and seasonal variation of moisture. These are briefly described in the following sub-sections.

2.1 Stresses

Stresses in the UGMs of the base and sub-base layers of pavements primarily originate from the moving traffic. The moving traffic load induces cyclic stresses of various magnitudes in the UGMs that consist of vertical, horizontal and shear components, shown in Figure 3. In this figure, σ_1 , σ_2 , σ_3 represent the principal stresses and σ_z is the vertical stress. For the UGMs, the vertical and horizontal stresses are compressive. The moving traffic load may result in shear stress reversal and rotation of the principal stresses (Lekarp 1999). The magnitude of the stresses in the pavement varies with depth depending on the stiffness of the different layers (Huang 2004). Some of the important factors that govern the stress conditions are the magnitude, volume and composition of the axle loads, tyre pressure and contact area (Wright 1996). The frequency of the loading is a function of the speed of the vehicles. Lateral wander of the traffic also has an impact on the stresses in the different layers (Wu and Harvey 2008, Erlingsson et al. 2012). An example of the lateral wander of traffic on a typical Swedish arterial road has been shown in Figure 4. Thus, the UGMs experience cyclic stresses of varying amplitudes occurring in a random order. Generally, the multilayer elastic theory, introduced by Burmister (1943, 1945), is widely used to compute the stresses in the different layers of pavements. Computer programs such as KENPAVE (Huang 2004), WinJulea (ARA 2004) and ERAPAVE (Erlingsson and Ahmed 2013) are available to aid in the computations. In Figure 5, a typical Icelandic low volume road structure is shown which was subject to Heavy Vehicle Simulator (HVS) tests in a study by Erlingsson (2002). Figure 6 shows the measured vertical stresses in that structure corresponding to a single wheel load of 60 kN with different tyre pressures and the results from the Finite Element (FE) analyses.

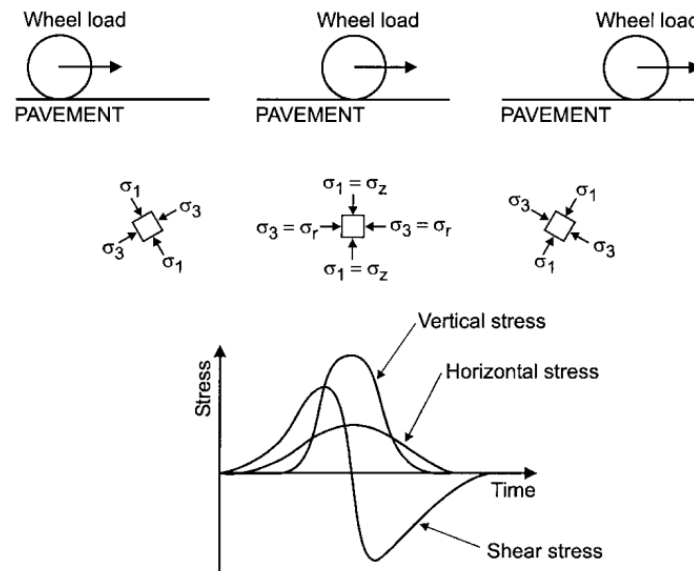


Figure 3. Stresses in UGMs due to moving wheel load (Lekarp 1999).

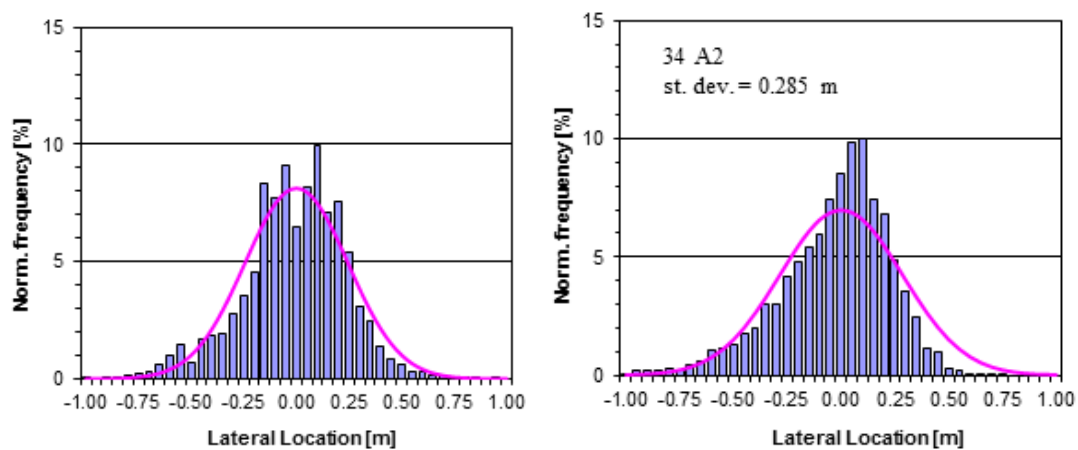


Figure 4. Lateral wander of traffic on a typical Swedish arterial road (Erlingsson et al. 2012)

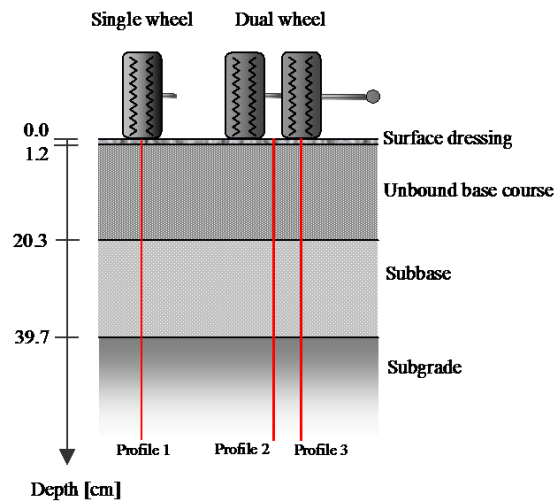


Figure 5. The pavement structure IS02, used for the HVS tests and FE analyses (Erlingsson 2002).

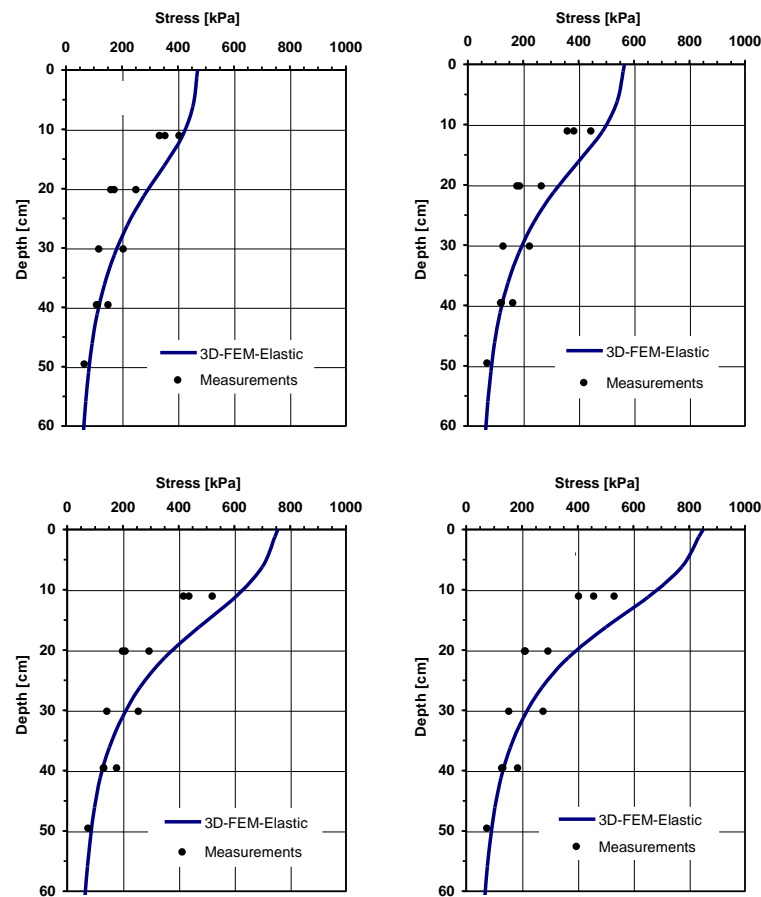


Figure 6. Comparison of measurements and FE analyses for IS 02 single wheel configuration, profile 1. The wheel load was in all cases 60 kN, whereas the tyre pressures were 500 kPa, 600 kPa, 800 kPa and 900 kPa, respectively (Erlingsson 2002).

2.2 Moisture

Moisture is known to have a major influence on the deformation behaviour of UGMs (Lekarp 1999, Erlingsson 2010, Cary and Zapata 2011). The presence of moisture generally increases the vulnerability of pavements to distress and failure when combined with traffic loading and freezing and thawing cycles. Well-designed pavements attempt to prevent accumulation of moisture in different layers by providing adequate drainage and cross-fall and by controlling the permeability of the different layers.

Along the length, pavements interact with various water phenomena. According to Erlingsson et al. (2009), these can be divided into three groups as (i) the road's own water which is the runoff due to precipitation, (ii) hinterland waters coming from the near-road environment (e.g. slopes from a cutting), and (iii) remote waters which have recharge areas far from the road but are crossing the road (e.g. rivers, groundwater flow, etc.). The water balance in pavements is complex and depends on the geometry and structure of the system (Erlingsson et al. 2009). Figure 7 illustrates an example of water balance in a pavement structure (Erlingsson et al. 2009).

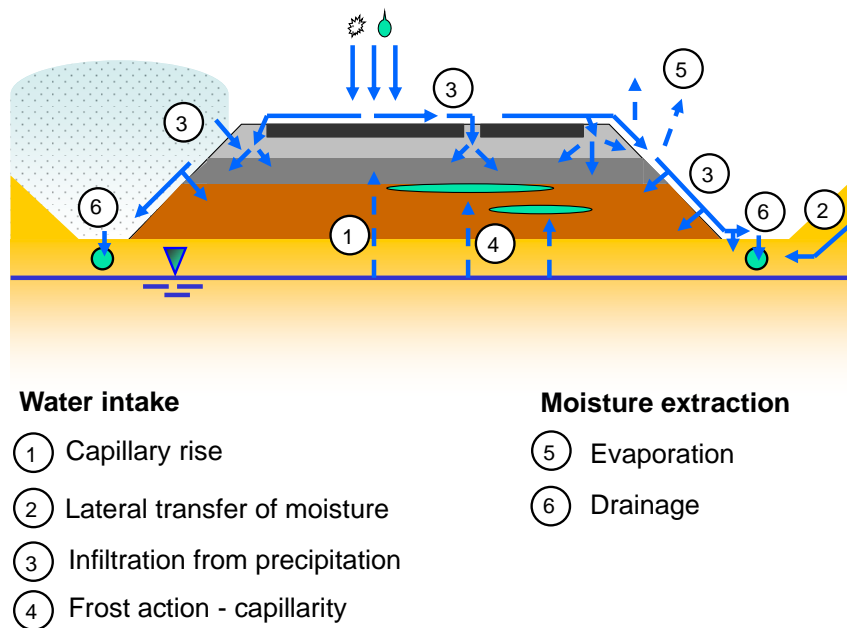


Figure 7. An illustration of moisture balance in a pavement structure (Erlingsson et al. 2009).

Moisture content in a pavement varies throughout the year depending on the climatic conditions. An example of the variation is shown in Figure 8. In cold regions, during the winter, pore water in the different layers forms ice lenses and increases the stiffness. During the spring thawing period, the ice lenses transform back to the liquid phase and get trapped within the surface course and the frozen or impermeable sub-layers. This results in excess moisture that has a great impact on the bearing capacity of the pavement (Salour and Erlingsson 2013). Thus, due to its great impact, the variation in the mechanical

properties of UGMs with seasonal variation of moisture needs to be taken into account in pavement design and management systems.

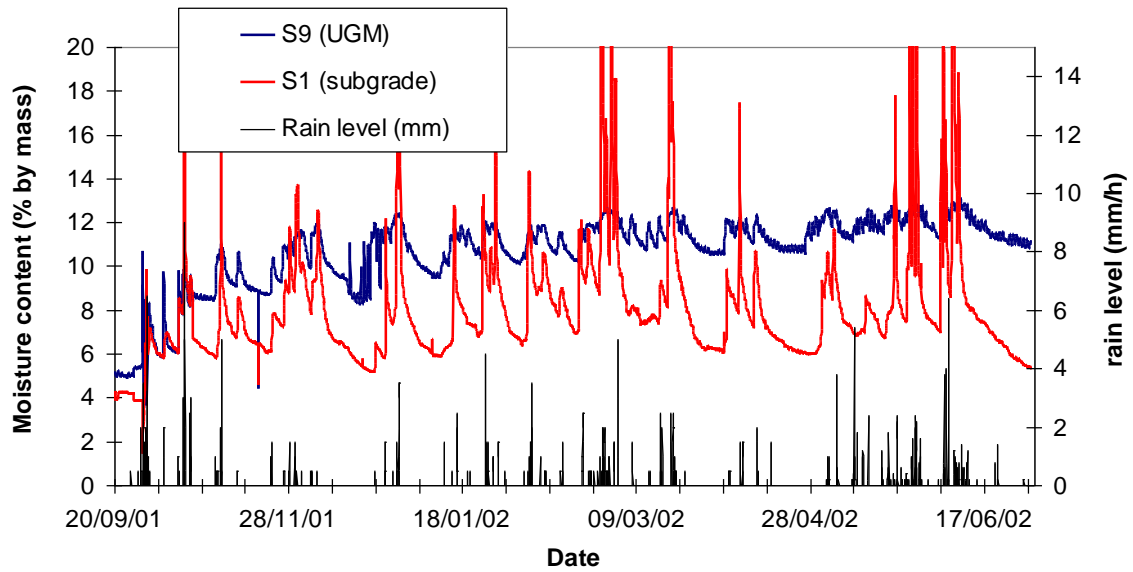


Figure 8. A typical variation in moisture content in the granular base and subgrade of a low traffic pavement (near the pavement edge) (Charlier et al. 2009).

3. DEFORMATION BEHAVIOUR OF UGMS

UGMs are an inhomogeneous aggregate of particles. The mechanical resistance of UGMs occurs mainly from particle interlocking and friction between the particles. The deformation behaviour of UGMs is characterized as anisotropic and complex elasto-plastic in nature (Kolisoja 1997, Uzan 1999, Erlingsson and Magnusdottir 2002). The total deformation due to compressive cyclic stresses in a UGM consists of two parts: (a) elastic or recoverable or resilient deformation (RD) and (b) irreversible or plastic or permanent deformation (PD). The RD is associated with the fatigue cracking of the AC layers while the PD results in rutting. For a single load pulse, this can be expressed as:

$$\varepsilon_{tot} = \varepsilon_r + \varepsilon_p \quad (1)$$

where ε_{tot} is the total axial strain, ε_r is the axial resilient strain and ε_p is the axial permanent strain, shown in Figure 9. Usually, the resilient strain is much larger than the permanent strain (Erlingsson and Magnusdottir 2002, El Abd et al. 2005). Both kinds of deformation in UGMs are non-linear stress dependent (Kolisoja 1997, Lekarp 1999, Englund 2011). Deformations occurring in UGMs have been attributed to consolidation, distortion and attrition (Lekarp, 1999). Consolidation is defined as the change in shape and compressibility of the particles, distortion is caused by bending, sliding and rolling of the individual particles, and attrition is the mechanism of breaking and crushing of the particles. Extensive studies on the deformation mechanisms of UGMs can be found in Kolisoja (1997).

The deformation behaviour of UGMs is influenced by several factors such as stress level, stress history, grain size distribution, moisture content, and degree of compaction.

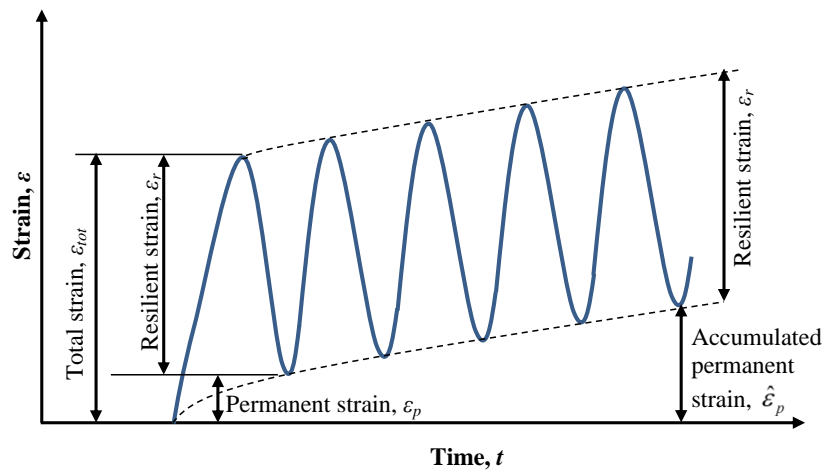


Figure 9. Strains in UGMs under cyclic loading.

3.1 RD characteristics

The RD in a UGM is proportional to the magnitude of stress and becomes stable after several load cycles of a constant magnitude (Huang 2004). The RD behaviour of UGMs is non-linear with respect to stress levels (Uzan 1985, Kolisoja 1997, Lekarp 1999, Englund 2011). Generally, the response of the material gets stiffer with increased stress level which has been termed as ‘strain hardening’ behaviour (Werkmeister 2003). This behaviour has been explained from a discrete perspective by Kolisoja (1997). In contrast, ‘strain softening’ behaviour is also observed in UGMs when shearing of the particles occurs (Englund 2011). The resistance of a UGM against RD is defined using the resilient modulus, M_R , which is an estimate of the stiffness modulus of the specimen for rapidly applied loads, expressed as (Huang 2004):

$$M_R = \frac{\sigma_d}{\varepsilon_r} \quad (2)$$

where σ_d (or q) is the cyclic deviator stress (stress in excess of the confining pressure). ε_r is taken after several load repetitions when the deformations are stabilized. M_R is an important parameter for pavement design. Generally, a higher M_R is desirable for better resistance against fatigue cracking of the AC layer. M_R is dependent on the state of stress, measured as the sum of the principal stresses, called the bulk stress, $\theta = \sigma_1 + \sigma_2 + \sigma_3$ or the mean normal stress or the hydrostatic stress, $p = \theta/3$. Other factors that affect M_R include density, grading, moisture content, stress history, aggregate type and shape (Lekarp 1999).

3.1.1 Modelling the RD behaviour with respect to stresses

The variation of M_R with θ can be expressed with the well-known k - θ model (Seed et al. 1962, Hicks and Monismith 1971, Uzan 1985) in its dimensionless form:

$$M_R = k_1 p_a \left(\frac{\theta}{p_a} \right)^{k_2} \quad (3)$$

where k_1 and k_2 are material parameters and p_a is a reference pressure usually taken as equal to the atmospheric pressure as 100 kPa. Several other variations of this model can be found in Uzan (1985), Uzan et al. (1992), Kolisoja (1997), Schwartz (2002), ARA (2004) and Araya (2011).

3.1.2 Influence of moisture on M_R

The M_R of UGMs has mostly been reported to decrease with increased moisture content (Lekarp 1999, Ekblad 2007, Salour and Erlingsson 2013). The effect of moisture on the stiffness of the sub-base UGM layer of a pavement section, back-calculated using falling weight deflectometer (FWD) data, is presented in Figure 10, showing that stiffness decreased when moisture content increased. This influence of moisture has been attributed

to the reduction of effective stresses due to the development of excess pore water pressure, lubrication effect of water, loss of internal friction, pumping of fines, degradation of the materials and loss of underlying supports (Lekarp 1999, Janoo 2002). However, the opposite trend was observed by Richter and Schwartz (2003). Dawson et al. (1996) have also reported that below the optimum moisture content, M_R tends to increase with increasing moisture. This has been explained as the effect of the development of suction (Dawson et al. 1996, Kolisoja 1997, Laloui et al. 2009). Above the optimum, with increased degrees of saturation, M_R is generally reported to decrease significantly (Dawson et al. 1996, Kolisoja 1997, Lekarp 1999).

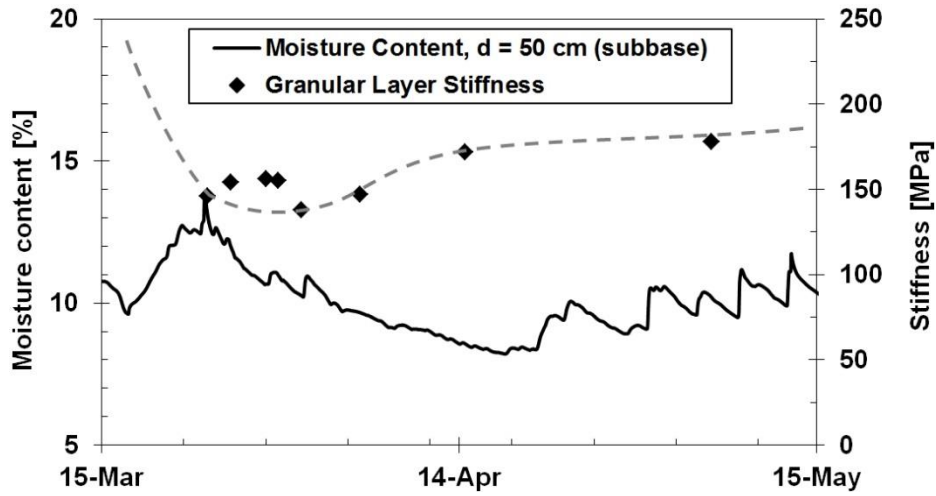


Figure 10. Variation in stiffness (back-calculated based on FWD measurements) with the variation of volumetric moisture content in a typical granular sub-base layer (Salour and Erlingsson 2013).

The current Mechanistic Empirical Pavement Design Guide (MEPDG) by AASHTO (The American Association of State Highway and Transportation Officials) uses the following model to characterize the effect of moisture on the M_R (ARA 2004):

$$\log_{10} \frac{M_R}{M_{Ropt}} = a + \frac{b - a}{1 + \exp \left[\ln \left(\frac{-b}{a} \right) + k_m (S - S_{opt}) \right]} \quad (4)$$

where

M_{Ropt} = Resilient modulus at optimum moisture content (w_{opt})

a = Minimum of $\log (M_R/M_{Ropt})$

b = Maximum of $\log (M_R/M_{Ropt})$

k_m = Regression parameter dependent on material properties

S = Degree of saturation expressed as decimal

S_{opt} = Degree of saturation at w_{opt} expressed as decimal.

Andrei (2003) proposed a simplified version of this model by eliminating density as a variable and using gravimetric moisture content (w) as the predictor variable instead of the degree of saturation (S). Cary and Zapata (2011) proposed another version of this model considering the matrix suction. Further aspects of the constitutive modelling of the influence of moisture can be found in Laloui et al. (2009).

3.2 PD characteristics

PD in UGMs accumulates with the number of load applications. Although, for each load cycle, PD is small compared to RD, it may accumulate to a significantly large value leading to rutting and eventual failure of the pavement, as shown in Figure 11. Development of PD is very much dependent on stress levels. It is directly related to deviator stress and inversely related to confining pressure (Morgan 1966). Several researchers have linked the development of PD to some form of stress ratio consisting of the deviator stress and the confining pressure (Lekarp 1999). Development of PD is also dependent on stress history where any previous history of loading reduces the accumulation of PD for a certain application of loading. A typical pattern of the development of PD for cyclic loading of a constant stress level is shown in Figure 12(a). However, if the stress level varies during the load applications, typically the case in real pavements, PD develops in the way as presented in Figure 12(b) due to the changes in the magnitudes of loading and the effect of stress history. The former case is simulated in the single stage (SS) RLT test while the latter case is simulated in the MS RLT test, discussed further in section 3.2.1.

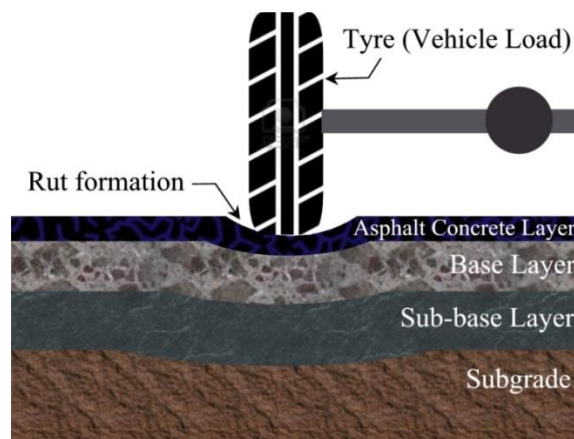


Figure 11. Development of rutting due to PD of the UGMs.

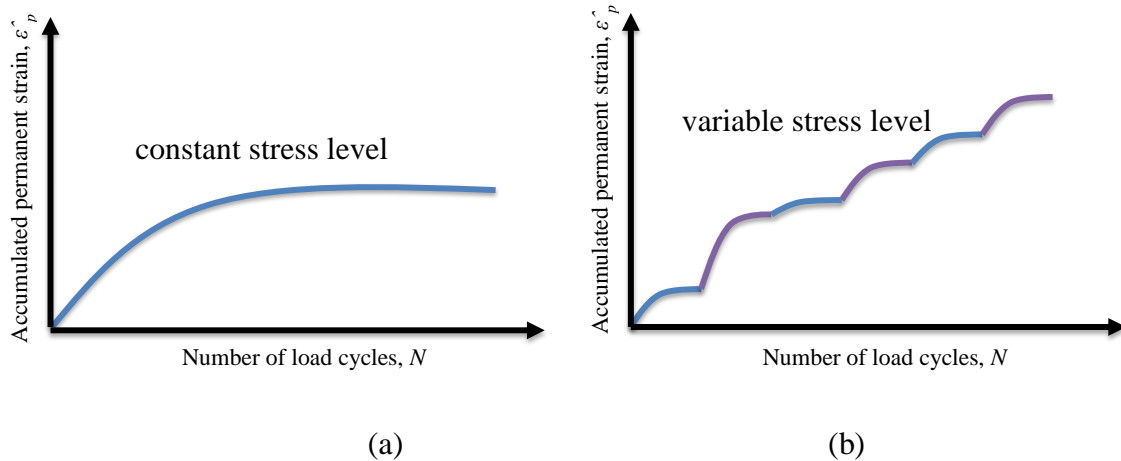


Figure 12. Development of PD at constant versus multiple stress levels.

To date, compared to RD properties, research regarding the PD behaviour of UGMs has been less extensive (Gidel et al. 2001, Uzan 2004, Hornych and El Abd. 2004). The occurrence of PD in UGMs has been attributed to compaction, crushing and material migration (Tholen 1980). It is found to develop in two phases. In the initial phase, PD increases rapidly with load applications due to post compaction accompanied by densification of the material, reduction in pore volume and volumetric change of the material (Werkmeister et al. 2004, El-Basyouny et al. 2005). The second phase is dominated by volume change. In this phase the deformation rate becomes more or less constant and shear deformation rises at an increasing rate (Werkmeister et al. 2004). At failure, only shear strain occurs with no volumetric change (El-Basyouny et al. 2005). Besides stress conditions, stress history and number of load applications, the other factors that have a major impact on the PD behaviour of UGMs are density, moisture content, grain size distribution and aggregate type (Lekarp 1999). The reorientation of the principal stresses in pavements has been reported to have some incremental effect on the accumulation of PD (Chan 1990).

Currently, the shakedown theory is being extensively used in recognizing different responses of UGMs under cyclic loading (Arnold 2004, Werkmeister et al. 2001, Werkmeister et al. 2004, Werkmeister 2006, and Tao et al. 2010). Based on this theory, Dawson and Wellner (1999) and Werkmeister et al. (2001) have identified that depending on stress levels, the evolution of PD in UGMs with the number of load cycles falls within the three shakedown ranges, shown in Figure 13. These ranges are described below in the order of ascending stress levels, where in each case, the stress level remains constant with the number of load applications:

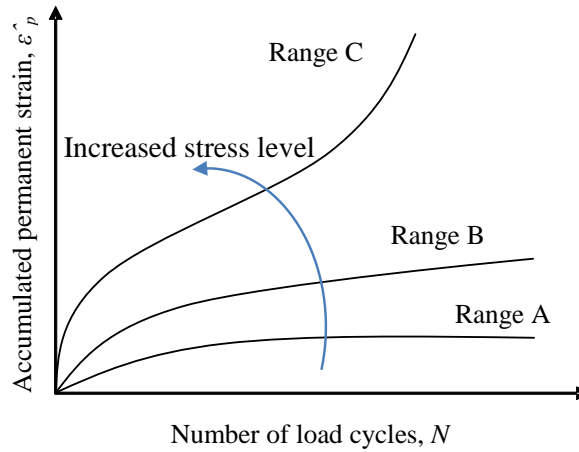


Figure 13. Different types of PD behaviour, depending on stress level (Dawson and Wellner 1999, Werkmeister et al. 2001).

- Range A - plastic shakedown range: For relatively low stress levels, permanent strain accumulates up to a finite number of load applications after which the response becomes entirely resilient and there is no further permanent strain. At this stage, the post-compaction is completed and the material is stabilized.
- Range B - intermediate response (plastic creep): For stress levels higher than that for range A, and up to a certain level, the accumulation of permanent strain continues with load applications. In this case, permanent strain rate (per cycle) decreases from high to a low and nearly constant level during the first load cycles.
- Range C - incremental collapse: When the stress levels are higher than that for range B, the permanent strain accumulates at a much faster rate compared to range A or B. In this case the permanent rate decreases very slowly or not at all. This may eventually lead to failure.

In a pavement structure, Range A behaviour is permitted to occur. Range B behaviour may be permitted for a limited number of load cycles and Range C behaviour should not appear at all (Werkmeister et al. 2001). For RLT tests, these shakedown boundaries can be defined using the following criteria (Werkmeister 2003, CEN 2004a):

$$\begin{aligned}
 \text{Range A: } (\hat{\epsilon}_p^{5000} - \hat{\epsilon}_p^{3000}) &< 0.045 \times 10^{-3} \\
 \text{Range B: } 0.045 \times 10^{-3} &< (\hat{\epsilon}_p^{5000} - \hat{\epsilon}_p^{3000}) < 0.4 \times 10^{-3} \\
 \text{Range C: } (\hat{\epsilon}_p^{5000} - \hat{\epsilon}_p^{3000}) &> 0.4 \times 10^{-3}
 \end{aligned} \tag{5}$$

where $\hat{\epsilon}_p^{3000}$ and $\hat{\epsilon}_p^{5000}$ are accumulated permanent strains at 3000th and 5000th load cycles, respectively, in the RLT test.

3.2.1 Modelling the PD behaviour with respect to stresses

Several models are available in the literature for describing the PD behaviour of UGMs. The earlier models can be divided into two types as (a) relationships describing the influence of the number of load applications and (b) relationships describing the influence of applied stresses (Lekarp 1999, Hornych and El Abd 2004). Relatively recent models combine the effect of stress with the number of load cycles. For this study, several of such recent models were chosen. However, the influence of other important factors such as moisture content, density, and grading are not directly taken into account by these models.

One of the models used here was proposed by Tseng and Lytton (1989), which was also included in the MEPDG (ARA 2004). It is expressed for an RLT test condition as:

$$\hat{\varepsilon}_p(N) = \varepsilon_r \varepsilon_0 e^{-\left(\frac{\rho}{N}\right)^\beta} \quad (6)$$

where $\hat{\varepsilon}_p(N)$ is the accumulated permanent strain after N number of load applications; ε_0 , ρ and β are material parameters and ε_r is the resilient strain at N^{th} load cycle. In this model, p and q are indirectly represented through ε_r .

The second model used in this study was developed by Gidel et al. (2001), expressed as:

$$\hat{\varepsilon}_p(N) = \varepsilon^0 \left[1 - \left(\frac{N}{100} \right)^{-B} \right] \left[\left(\frac{L_{\max}}{p_a} \right)^u \left(m + \frac{s}{p_{\max}} - \frac{q_{\max}}{p_{\max}} \right)^{-1} \right] \quad (7)$$

where ε^0 , B and u are material parameters, $L_{\max} = \sqrt{p_{\max}^2 + q_{\max}^2}$ and p_{\max} and q_{\max} are the maximum applied hydrostatic stress and deviator stress, respectively, m is the slope, and s is the intercept of the Mohr-Coulomb failure line in p - q space, ideally determined using static failure triaxial tests.

The third model used here is the one proposed by Korkiala-Tanttu (2005). This model expresses the accumulated permanent strain $\hat{\varepsilon}_p(N)$ after N number of load cycles as:

$$\hat{\varepsilon}_p(N) = CN^b \frac{R}{A - R} \quad (8)$$

where C and b are material parameters. A is a material independent parameter taken as 1.05. R is the ratio of the applied deviator stress to the deviator stress at failure, determined using static triaxial tests.

Usually, the material parameters of these models are evaluated by running RLT tests where load pulses of a constant magnitude are applied to a specimen for about 80,000 to 100,000 cycles. This is referred to as the SS RLT test (CEN 2004a). To study the influence of

different stress levels on the material, each time a new SS RLT test on a new specimen needs to be run. In this case, the effect of stress history on the material cannot be studied. On the other hand, the MS RLT test (CEN 2004a) applies several stress paths to a single specimen and thus (a) it includes the effect of stress history, (b) reduces the time and effort required to study the influence of several stress levels and (c) reduces the experimental scatter usually experienced in testing several specimens. Furthermore, it should be more reliable to evaluate the material parameters of a model from a large number of stress paths in MS RLT tests. Hence, for a comprehensive study of the material behaviour, the MS RLT test is the more convenient option. However, the modelling of the PD behaviour in this case becomes more complex. In fact, the current PD models cannot be directly applied to MS RLT tests for the reason explained in the following paragraph.

In an MS RLT test, if the stress level is increased after a certain number of load cycles N_1 , by applying a different stress path to the same specimen, the accumulation of permanent strain continues along the curve AC, after it had been accumulated to $\hat{\epsilon}_{p1}$ along the line OA for the first stress path, as shown in Figure 14. The total accumulated permanent strain will be $\hat{\epsilon}_{p2}$ at the end of the total number of load cycles N_2 . If only stress path 2 was applied to the specimen, it would have developed along the line OEBFD, resulting in the total accumulated permanent strain of $\hat{\epsilon}_{p2'}$. Since, in the MS loading condition, the material has already experienced the accumulated strain $\hat{\epsilon}_{p1}$ because of the load history from stress path 1, the continuing strain for stress path 2 will follow the path similar to EBF. This is the path the material would have followed after $\hat{\epsilon}_{p1}$ for the second stress path alone. In this case, point E will be shifted to point A where it will start to accumulate after N_1 load cycles. Thus the paths EBF and AC should be identical. For modelling, using any of the models similar to those described in this section, if the input of the stress level is changed after N_1 for stress path 2, the model will predict the path BFD for this stress path which will result in the deformation curve of OABFD instead of OAC with the total accumulated permanent strain of $\hat{\epsilon}_{p2'}$ instead of the actual $\hat{\epsilon}_{p2}$. Thus some modification is required to implement these models for an MS loading condition. This modification was proposed in Paper II based on the time-hardening concept, introduced by Lytton et al. (1993).

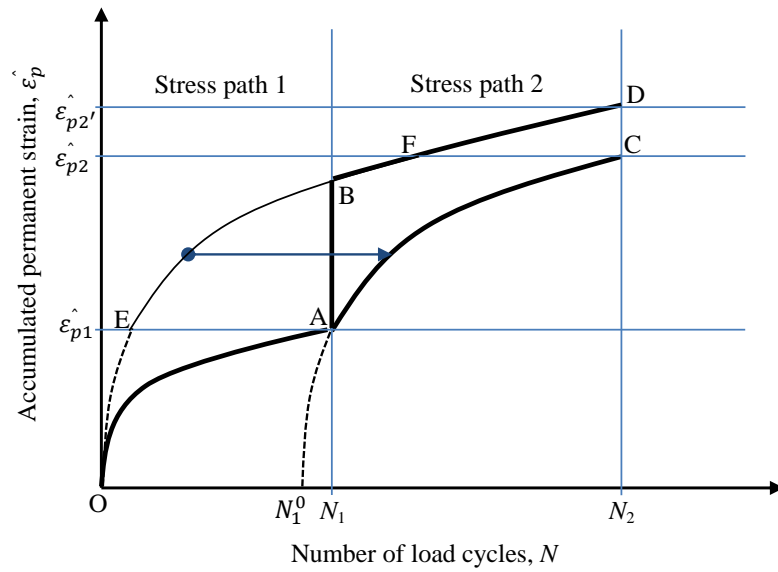


Figure 14. Effect of stress history in modelling the accumulation of PD in MS RLT tests.

3.2.2 Influence of moisture on PD

The presence of moisture increases PD in UGMs (Lekarp 1999). According to Thom and Brown (1987), PD may increase dramatically for a relatively small increase in moisture content. They have reported that the lubrication effect of moisture is the primary influencing factor. Researchers generally agree that when there is a high degree of saturation and low permeability, PD increases with moisture due to an increase in pore water pressure, thus reducing the effective stress, which in turn, lowers the stiffness and deformation resistance of the material (Lekarp 1999). The effect of moisture on the accumulation of PD is shown in Figure 15. The data are from an HVS test section where the ground water table was raised after about 500,000 load repetitions, shown in the figure with a vertical line. This clearly shows that PD started to increase with the introduction of water. However, any well-established model to mathematically describe the influence of moisture on the PD behaviour of UGMs is still lacking.

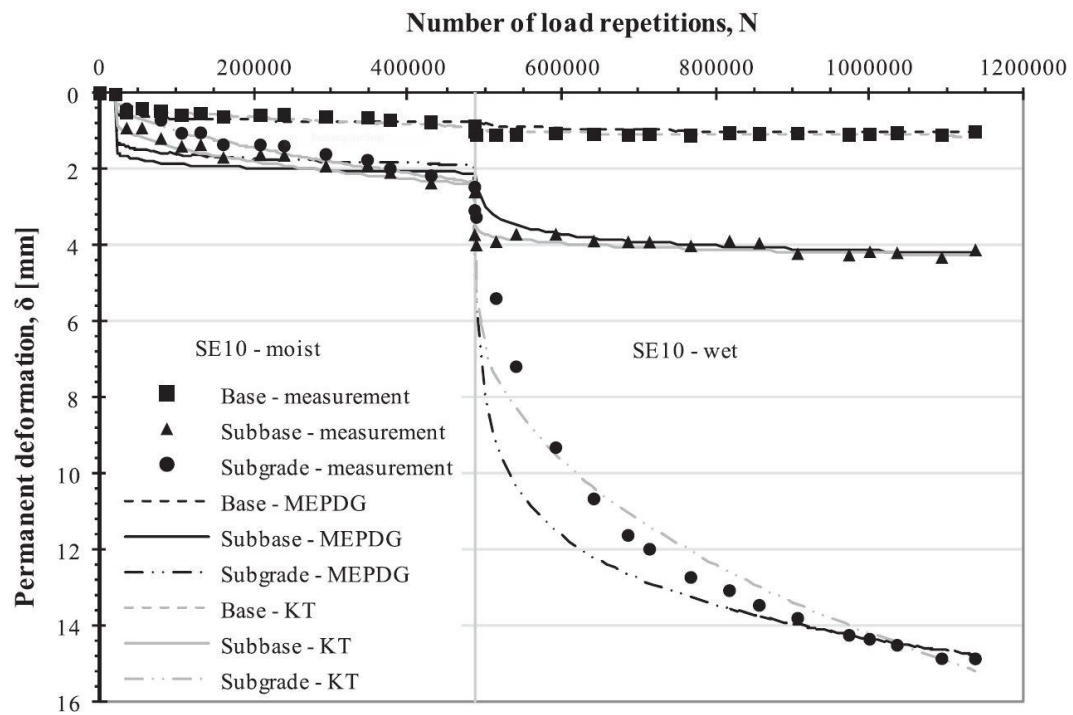


Figure 15. Effect of moisture on the accumulation of PD in an HVS test section. The vertical line indicates the introduction of water (Saevarsdottir and Erlingsson 2013).

4. EXPERIMENTAL STUDY

This study was based on RLT tests performed on several UGMs typically used in base layers of flexible pavements in Sweden and Denmark. The tests were carried out following the European standard EN-13286-7 (CEN 2004a). Specimens with a range of moisture content, different grain size distributions and different stress levels were tested with specific objectives, described in the appended papers.

4.1 The RLT test

For characterizing the deformation behaviour of UGMs, the RLT test is considered to be the most convenient way (Lekarp 1999). The RLT test simulates the cyclic stresses similar to those experienced by the UGMs in the field and applies these stresses to a prepared cylindrical specimen, as shown in Figure 16. The resulting deformations in the specimen are then measured, from which the RD and PD characteristics of the material are evaluated. In an RLT test, the cylindrical specimen is subjected to cyclic stresses consisting of confining pressure, σ_c (either cyclic or constant) and a cyclic deviator stress, σ_d or q . Thus, the principal stresses acting on the specimen are: $\sigma_1 = \sigma_3 + \sigma_d$ (total axial stress), and $\sigma_2 = \sigma_3 = \sigma_c$. The bulk stress is then, $\theta = \sigma_1 + 2\sigma_3$.

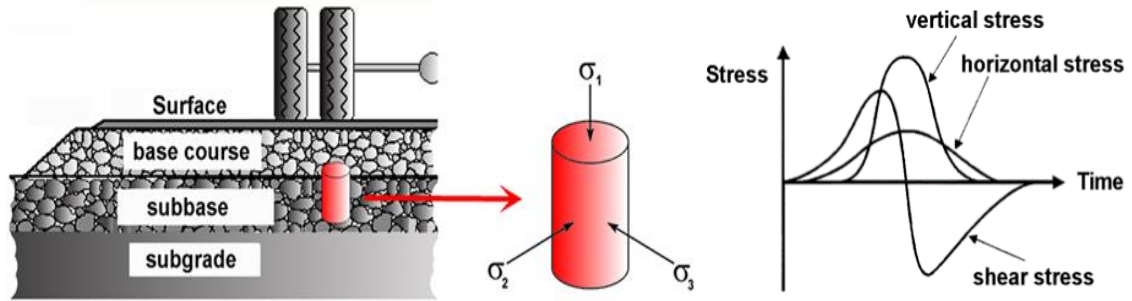


Figure 16. Principles of the RLT test (Erlingsson and Magnusdottir 2002).

For the study of the RD characteristics, the RLT tests are generally carried out by applying several stress paths for a relatively small number of cycles on a single specimen. Then from the measured RDs and stress levels, the values of M_R are plotted as a function of θ or p . Since in the RD tests a limited number of load cycles are applied, any effect due to post-compaction and accumulated PD may be neglected. This allows for the study of the pure resilient behaviour of the materials.

For the study of the PD behaviour, the load pulses are applied for a relatively large number of cycles. This usually results in a considerable amount of accumulated PD and PC. The measured PDs are generally plotted as the accumulated function of N . As discussed in section 3.2.1, there are two versions of the PD test: (a) the SS RLT test and (b) the MS

RLT test. From an MS RLT test it is also possible to evaluate the RD properties of the material. In this case the effect of post-compaction is larger than that of the RD tests.

The RLT test makes some simplifications to the in-pavement stress situations. For instance, shear stresses are more complex in reality due to the effect of the rotation of the principal stress axes and the lateral wander of traffic (Correia and De Almeida 1998, Lekarp 1999, Araya 2011). The RLT test equipment with constant confining pressure cannot simulate these effects. Although these may be partly simulated using the RLT test with cyclic confining pressure or by specialized hollow cylinder test (Araya 2011, Qiao et al. 2014), these test methods have some inherent drawbacks. Generally, the RLT test reveals a great deal of information regarding the mechanical behaviour of the materials and is the most widely used test method available (Gidel et al. 2001). Because of the simplifications, the models and the material parameters derived using the RLT test may need to be modified to implement them for in situ conditions.

4.2 Description of the equipment

The RLT test equipment used for this study, shown in Figure 17, conforms to the European standard (CEN 2004a). The triaxial cell of a plexiglass cylinder is designed for cylindrical specimens of 150 mm in diameter and 300 mm in height to be placed inside. The cell is equipped with drainage systems at the top and bottom. During the preparation of the specimen, a porous disk is placed at the bottom to facilitate drainage. The axial load sensor (20kN) is placed inside the cell with the loading piston. The confining pressure is generated using compressed air. A pressure sensor is located inside the cell to measure the confining pressure which can be controlled through a pneumatic system. The specimen is always prepared inside a thin rubber membrane that seals the material from the compressed air for the confining pressure to be effective and the measurements to be accurate. The axial deformations of the specimen are measured using three linear variable displacement transducers (LVDTs). These are mounted on the middle third of the specimen, maintaining 120° angles among them. The gauge length is then 100mm. The LVDTs are attached to the specimen by screwing them to anchors (studs) placed inside the specimen during compaction. These studs were developed in accordance with the study carried out by Anderi (2003) and their size is related to the maximum particle size that can be tested using this RLT test setup. Prior to the preparation of the specimen, the studs are mounted on the wall of the cylindrical mould (in which the specimen is compacted) with screws, producing the gauge length of 100mm with 120° angles among the LVDT axes. After the compaction of the specimen, the screws are taken off and the specimen is extracted from the mould leaving the anchors inside and maintaining their proper positions. The LVDT holders are then fixed from the outside of the membrane by puncturing the membrane and screwing them to the studs. Then the LVDTs are mounted to the holders. Figure 18 shows the studs, the LVDT holders and the studs mounted inside the cylindrical mould before the specimen preparation. Since the membrane is punctured during installation of the LVDTs, caulking is applied around the LVDT holders to prevent any air leakage. There is another LVDT

attached to the loading piston, outside the triaxial cell that measures the total axial deformation of the specimen. However, measurements from this LVDT were not reported in this study. This is generally used as a control for the internal LVDTs. The system is also capable of measuring the radial deformations at mid-height of the specimen, using an extensometer attached directly to the specimen with a belt. The axial loading system is a servo-hydraulic loading mechanism, shown in Figure 19. The hydraulic system and data acquisition are controlled by a computer. The signals from the gauges are fed to the computer via signal conditioners. All the necessary excitations for the gauges are also provided by the signal conditioners.

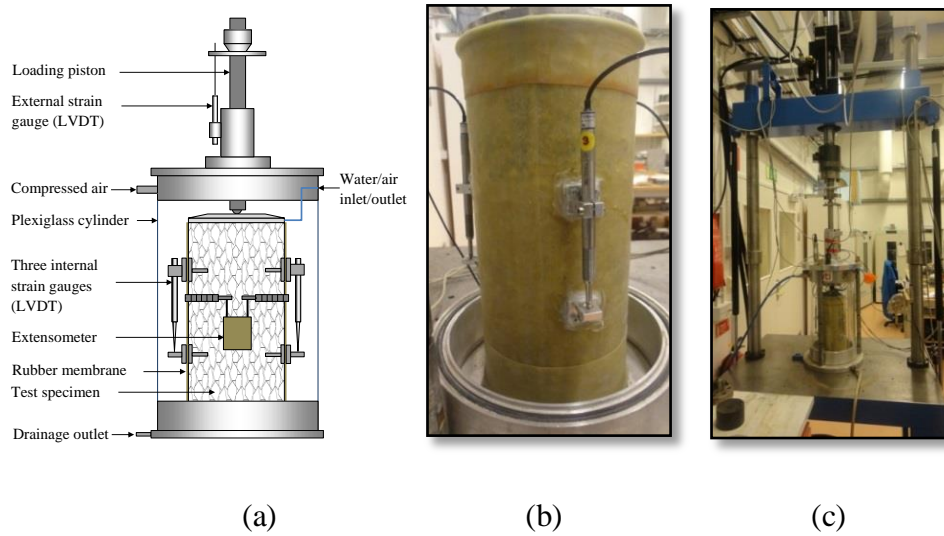


Figure 17. (a) Schematic overview of the triaxial test cell, (b) axial LVDTs mounted on the specimen, (c) triaxial cell placed in the loading frame.

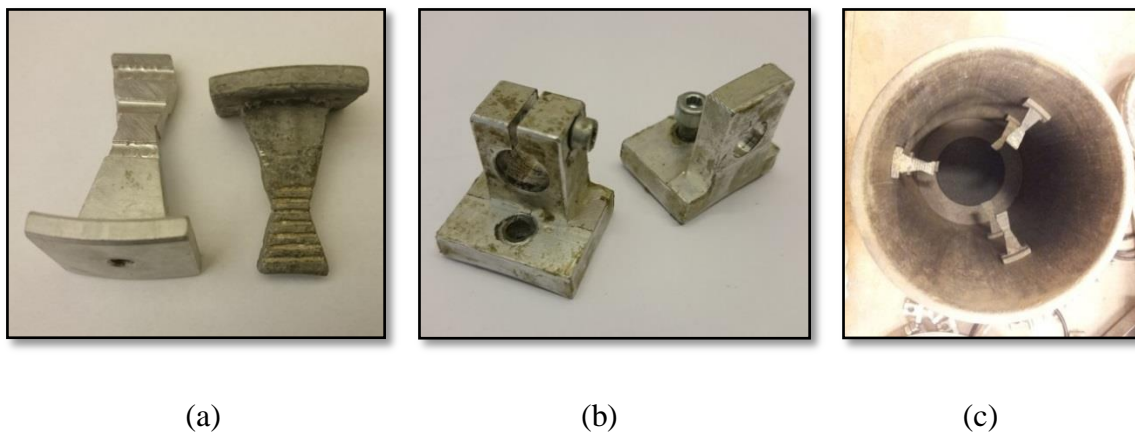


Figure 18. (a) The studs that are placed inside the specimen, (b) the LVDT holders, (c) the studs mounted inside the cylindrical mould before preparation of the specimen.

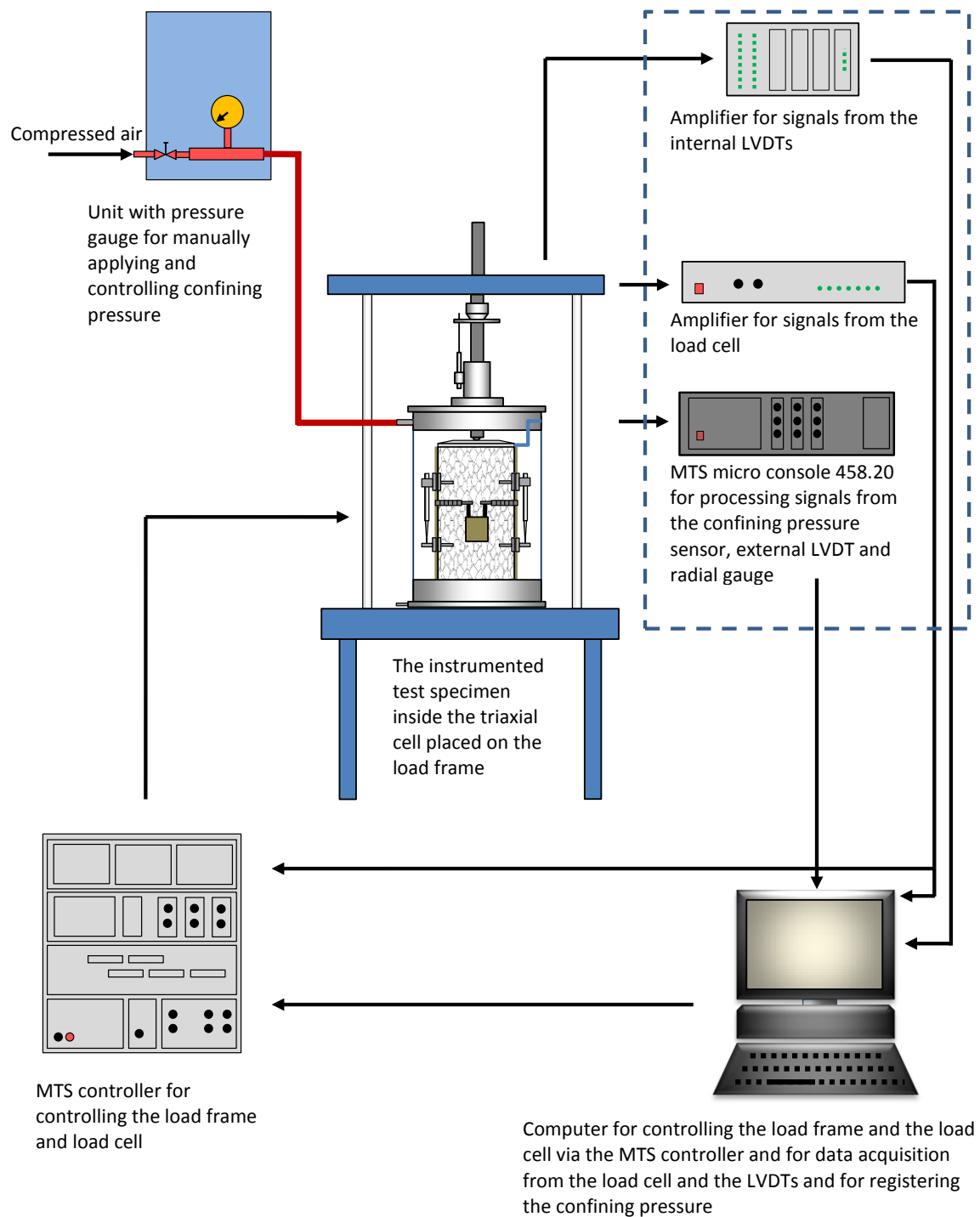


Figure 19. Schematic of the servo-hydraulic RLT test system.

4.3 Specimen preparation

First, the materials were sieved and the different particle sizes were mixed in proportion to achieve the desired grain size distributions. The optimum moisture content and the maximum dry density were determined using the Proctor compaction method, as described by the European standard (CEN 2004b). The specimens were prepared using a fixed

volume cylinder of 5.3 litres which produces cylindrical specimens of the size 150 mm in diameter and 300 mm in height. For the volume of the cylinder, to achieve the target dry density, the required mass of the dried material was calculated. Then the required amount of material was mixed thoroughly with the required amount of water to achieve the target moisture content. Most of the mix was then poured into the cylindrical mould of the vibrocompactor, shown in Figure 20 (a). The mould was previously prepared with the anchors for LVDTs, porous disk and bottom plate. Then the mould was placed inside the vibrocompactor where the rest of the material was put in the removable extended part of the cylinder. The material was then compacted by the vibrocompactor using a static hammer load and simultaneous shaking, which forced all of the material to get inside the fixed volume cylinder. Thus this process yielded specimens with the desired dry densities and moisture contents. After compaction, the top plate and the membrane were put on the cylinder and were secured with O rings. The specimen was then extracted from the cylinder using a hydraulic jack, shown in Figure 20 (b).

After extraction, the LVDTs were mounted onto the specimen and the setup was placed inside the triaxial chamber where all the electrical and drainage connections were made. The chamber was then closed and the system was left overnight to obtain an even distribution of moisture inside the specimen and the caulking to be dried. If it was not possible to prepare a specimen with high moisture content, it was prepared at lower moisture content and water was added later and was left for a few hours to reach a uniform moisture distribution.



(a)



(b)

Figure 20. Specimen preparation: (a) vibrocompaction, (b) hydraulic extraction (Arvidsson 2006).

4.4 Test procedure

The RLT tests were carried out in accordance with the European standard EN-13286-7 (CEN 2004a). In all cases, the constant confining pressure method was used. To study the resilient properties, the test procedure for resilient modulus was followed. To study the PD properties, the MS loading method was adopted. The stress levels were selected from the tables provided in the European standard. For the resilient tests, only the high stress level (HSL), shown in Table 1, was used. For the PD tests, both the HSL and low stress level (LSL), shown in Table 2 and Table 3 respectively, was used depending on the objective. During the tests, each stress path was applied for 100 cycles for the resilient tests and 10,000 cycles for the PD tests. For the resilient tests, the specimens were conditioned before testing by applying loading pulses with a maximum deviator stress of 340 kPa for 20,000 cycles with a constant confining pressure of 70 kPa, as prescribed by the standard. In Figure 21, the state of stress in the triaxial cell and the stress paths for the PD tests using HSL and LSL according to the European standard are shown.

Table 1. Stress levels used for the resilient modulus tests (CEN 2004a).

High stress level											
Confining stress, σ_3 kPa	Deviator stress, σ_d kPa		Confining stress, σ_3 kPa	Deviator stress, σ_d kPa		Confining stress, σ_3 kPa	Deviator stress, σ_d kPa		Confining stress, σ_3 kPa	Deviator stress, σ_d kPa	
constant	min	max	constant	min	max	constant	min	max	constant	min	max
20	0	30	35	0	50	50	0	80	70	0	115
20	0	50	35	0	80	50	0	115	70	0	150
20	0	80	35	0	115	50	0	150	70	0	200
20	0	115	35	0	15	50	0	200	70	0	280
-	-	-	35	0	200	50	0	280	70	0	340
Confining stress, σ_3 kPa	Deviator stress, σ_d kPa		Confining stress, σ_3 kPa	Deviator stress, σ_d kPa							
constant	min	max	constant	min	max						
100	0	150	150	0	200						
100	0	200	150	0	280						
100	0	280	150	0	340						
100	0	340	150	0	400						
100	0	400	150	0	475						

Table 2. Stress levels used for the PD tests (HSL) (CEN 2004a).

High stress level														
Sequence 1			Sequence 2			Sequence 3			Sequence 4			Sequence 5		
Confining stress, σ_3 kPa	Deviator stress, σ_d kPa		Confining stress, σ_3 kPa	Deviator stress, σ_d kPa		Confining stress, σ_3 kPa	Deviator stress, σ_d kPa		Confining stress, σ_3 kPa	Deviator stress, σ_d kPa		Confining stress, σ_3 kPa	Deviator stress, σ_d kPa	
constant	min	max	constant	min	max	constant	min	max	constant	min	max	constant	min	max
20	0	50	45	0	100	70	0	120	100	0	200	150	0	200
20	0	80	45	0	180	70	0	240	100	0	300	150	0	300
20	0	110	45	0	240	70	0	320	100	0	400	150	0	400
20	0	140	45	0	300	70	0	400	100	0	500	150	0	500
20	0	170	45	0	360	70	0	480	100	0	600	150	0	600
20	0	200	45	0	420	70	0	560						

Table 3. Stress levels used for the PD tests (LSL) (CEN 2004a).

Low stress level														
Sequence 1			Sequence 2			Sequence 3			Sequence 4			Sequence 5		
Confining stress, σ_3 kPa	Deviator stress, σ_d kPa		Confining stress, σ_3 kPa	Deviator stress, σ_d kPa		Confining stress, σ_3 kPa	Deviator stress, σ_d kPa		Confining stress, σ_3 kPa	Deviator stress, σ_d kPa		Confining stress, σ_3 kPa	Deviator stress, σ_d kPa	
constant	min	max	constant	min	max	constant	min	max	constant	min	max	constant	min	max
20	0	20	45	0	60	70	0	80	100	0	100	150	0	100
20	0	40	45	0	90	70	0	120	100	0	150	150	0	200
20	0	60	45	0	120	70	0	160	100	0	200	150	0	300
20	0	80	45	0	150	70	0	200	100	0	250	150	0	400
20	0	100	45	0	180	70	0	240	100	0	300	150	0	500
20	0	120	45	0	210	70	0	280	100	0	350	150	0	600

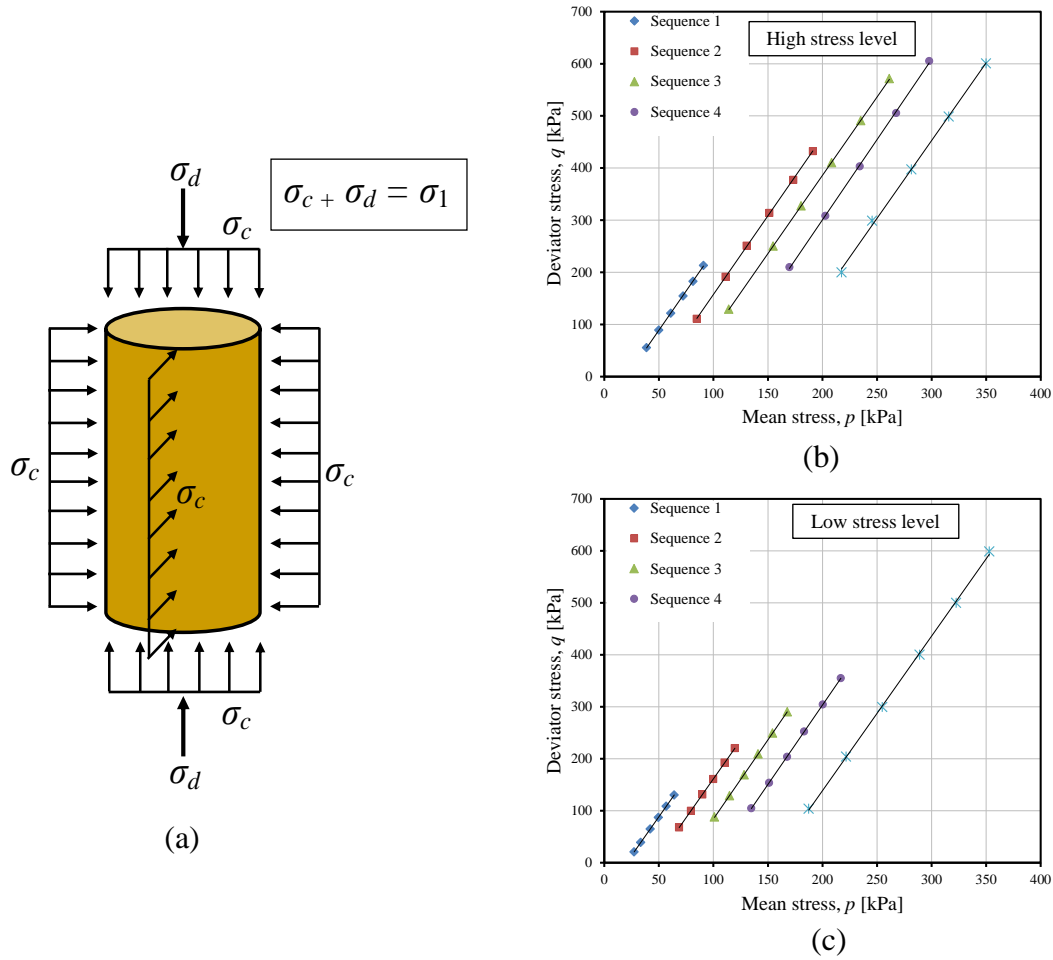


Figure 21. (a) Stress state in the triaxial cell, (b) stress paths for HSL, (c) stress paths for LSL.

The cyclic loading used for the tests were haversine pulses with a frequency of 10 Hz without any rest period. This is within the specification of the European standard. Since load duration and frequency do not have any significant influence on the deformation behaviour of UGMs (Lekarp 1999), this loading pattern was selected to speed up the process. An example of the load pulse and corresponding axial deformation is shown in Figure 22.

During the tests, for each sequence the confining pressure was controlled manually and the cyclic loading was controlled by the computer. For this equipment, to maintain contact of the loading piston to the specimen, the minimum deviator stress during cyclic loading σ_{dmin} was set to 3 kPa. An example of stress versus strain plots for a few cycles of loading of $\sigma_d = 280$ kPa with $\sigma_3 = 70$ kPa is shown in Figure 23.

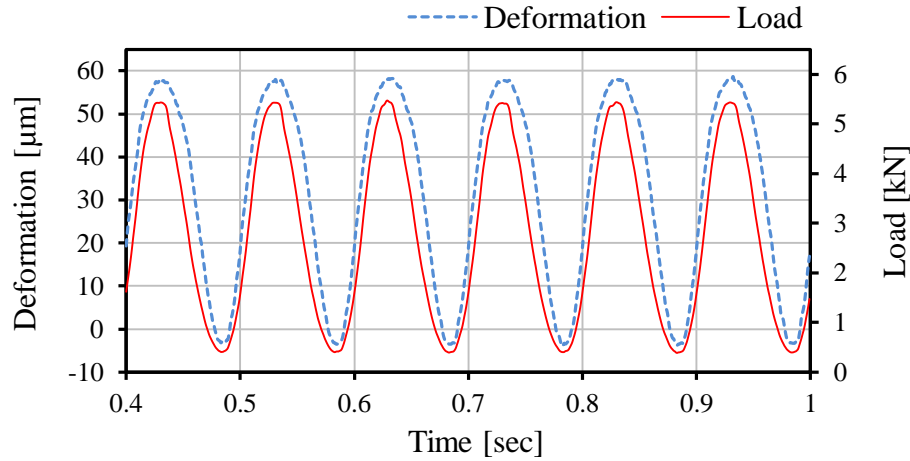


Figure 22. A typical registration of six load pulses and corresponding deformations.

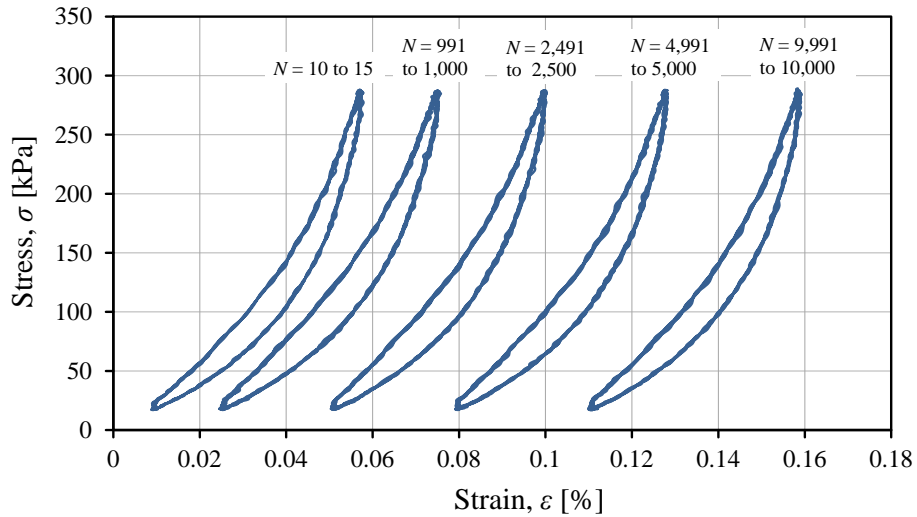


Figure 23. Typical stress versus strain plots for a few cycles of loading in a PD test ($\sigma_d = 280$ kPa, $\sigma_3 = 70$ kPa).

Several static failure triaxial tests were performed using the same triaxial test setup. For this, three identical specimens of a UGM of interest were prepared. Each of these specimens was then subjected to a monotonic increase in strain at the rate of 1%/min, using confining pressure levels of 10, 20 and 40 kPa respectively and the deviator stress at failure q_f for these specimens were identified. These were later used to determine the shear strength parameters m and s of the specimen.

After each test, moisture content of the specimen was measured. The measured final moisture contents were a little less than the initial because of some losses due to drainage. For this study, only the target (initial) moisture contents have been reported. The degree of compaction was also checked.

4.5 Materials used and tests performed

The UGMs used for this study were originated in Sweden and Denmark. These materials are commonly used in the base and sub-base layers of flexible pavements in these countries. The Swedish UGMs, referred to as Skärlanda, Hallinden, SPV and VKB, are crushed rock aggregates. The Danish UGMs, referred to as Siem and SG1, are blends of natural aggregates with crushed fractions derived from crushing of the oversized stones. Pictures of these aggregates are shown in Figure 24. The grain size distributions of these materials were those typically used for base layers. In addition, three different grain size distributions (derived using the Fuller's equation where the values of n represent the grading coefficients) of the Skärlanda aggregates were used. The objective was to study the degree of impact of moisture on the different grain size distributions covering a relatively broad range of grain size distributions. The grain size distribution curves of the materials are presented in Figure 25. The maximum size of the particles used for the tests was 31.5 mm.

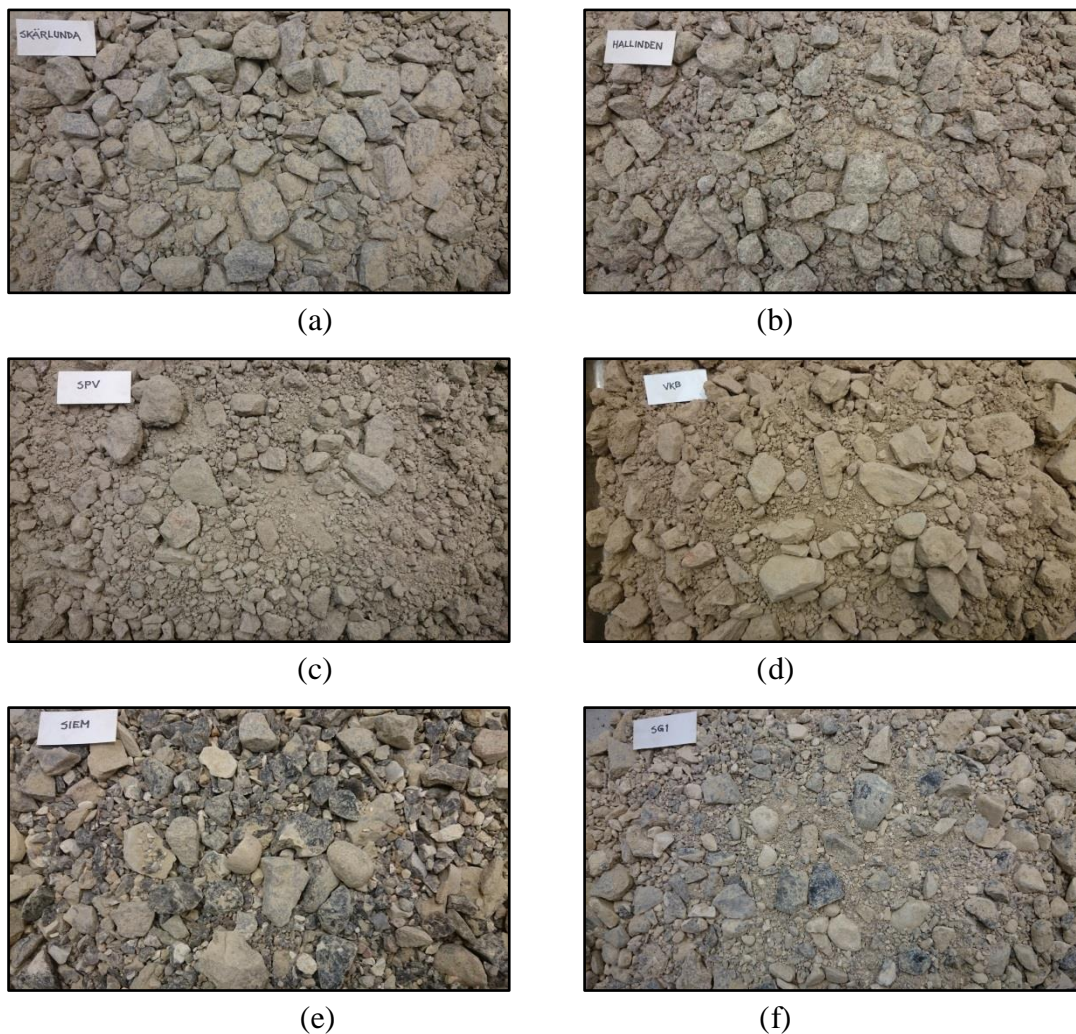


Figure 24. Pictures of the UGMs tested: (a) Skärlanda, (b) Hallinden, (c) SPV, (d) VKB, (e) Siem, (f) SG1.

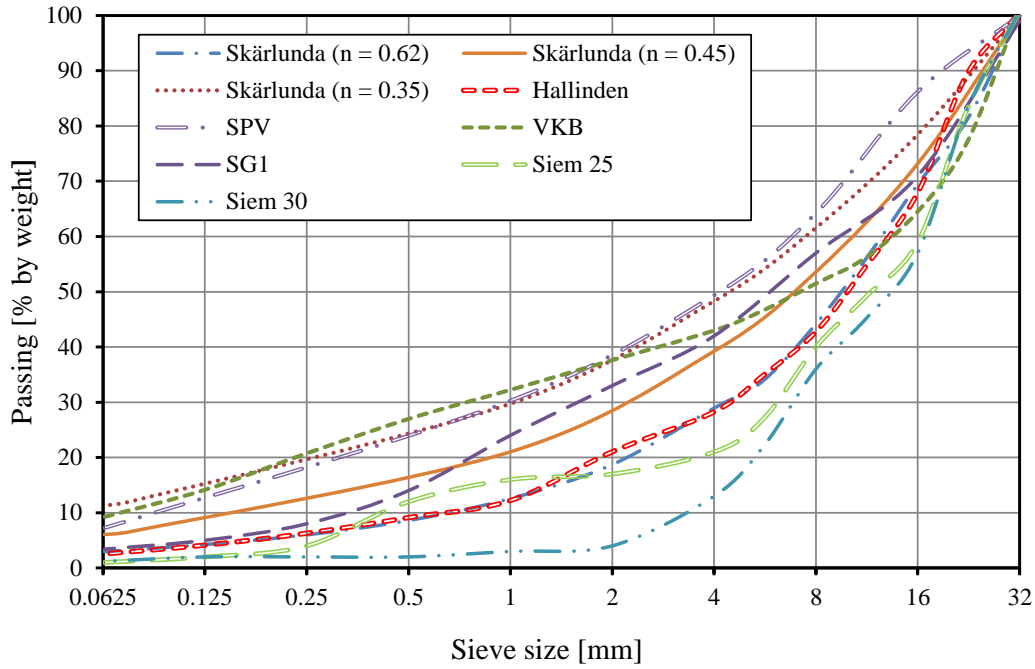


Figure 25. Grain size distribution curves of the UGMs tested.

Generally, all the materials were tested for specific gravity, grain size distribution (sieve analysis), the optimum moisture content and the maximum dry density. The tests for the optimum moisture content and the maximum dry density using the modified Proctor method were performed by the author. On the other hand, the tests using the standard Proctor method, as reported in some of the appended papers, were performed by the Danish Road Directorate. For some of the UGMs, the shear strength parameters were evaluated using static failure triaxial tests. Different types of RLT tests were performed using the different materials depending on the objectives, as listed in Table 4, Table 5 and Table 6.

The degrees of saturation (S) of the specimens were calculated using the following formula:

$$S = \frac{w}{\left(\frac{G_s \gamma_w}{\gamma_{dry}} - 1 \right)} \quad (9)$$

where G_s is the specific gravity of the particles, γ_w is the dry unit weight of water and γ_{dry} is the dry density of the test specimen.

Most of the RLT tests were replicated to account for any experimental scatter. It should be mentioned here that some replications of the tests were performed after the publication of some of the papers and the data were improved based on these replications in the subsequent papers.

Table 4. List of the RD (RLT) tests performed.

Material	G_s [-]	Fines ($<0.075\text{mm}$) content [%]	w_{opt} [%]	S_{opt} [%]	w_{sat} [%]	Maximum dry density [gm/cc]	Test conditions			
							γ_{dry} [gm/cc]	Range of w [%]	Range of S [%]	Samples tested
Skärlunda ($n = 0.62$)	2.64	2.4	5.5	50.5	11	2.11	2.05	1-8	9-73	3
Skärlunda ($n = 0.45$)	2.64	6.5	6.0	77.1	7.8	2.26	2.19	1-7.5	12-96	1
Skärlunda ($n = 0.35$)	2.64	12	6.5	75.3	8.7	2.22	2.15	1-8	11-92	2
VKB	2.54	10.2	6.0	95.4	6.3	2.21	2.19	2-6.2	31-98	1
SPV	2.68	8.6	6.9	91.6	7.6	2.35	2.23	2-7.5	26-99	1
SG1	2.49	3.8	7.5	90.9	9.4	2.14	2.02	3.5-9.2	37-98	2

Table 5. List of the PD (RLT) tests performed.

Material	Fines content ($< 0.075\text{mm}$) [%]	w_{opt} [% by weight]	G_s [-]	Maximum dry density [gm/cc]	Tests performed with				
					w [% by weight]	S [%]	γ_{dry} [gm/cc]	Stress level	Samples tested
Skärlunda ($n = 0.62$)	2.4	5.5	2.64	2.11	1	9.1	2.05	HSL	2
					3	27.3	2.05	LSL	2
					3	27.3	2.05	HSL	2
					5	45.5	2.05	HSL	2
					5.5	45.4	2.00	LSL	1
					5.5	45.4	2.00	HSL	2
					7	63.8	2.05	HSL	2
Skärlunda ($n = 0.45$)	6.5	6	2.64	2.26	1	12.9	2.19	HSL	2
					3	38.8	2.19	HSL	2
					5	64.6	2.19	HSL	2
					6.5	84.0	2.19	HSL	2
Skärlunda ($n = 0.35$)	12	6.5	2.64	2.22	1	11.7	2.15	LSL	3
					1	11.7	2.15	HSL	2
					2	23.4	2.15	HSL	2
					3.5	40.9	2.15	HSL	2
					5	58.4	2.15	HSL	1
					6	70.1	2.15	HSL	2
Skärlunda ¹	1.9	5	2.64	2.075	3	23.3	1.97	LSL	1
Hallinden	2.2	5.5	2.63	2.075	1	8.6	2.01	LSL	1
					3.5	30.0	2.01	LSL	2
					5.5	47.2	2.01	LSL	2
					6.5	55.7	2.01	LSL	2
VKB	10.2	6	2.54	2.21	2	31.6	2.19	LSL	2
					4.5	71.0	2.19	LSL	3
					4.5	71.0	2.19	HSL	1
					6	94.7	2.19	LSL	2

(continued on next page)

Table 5 (continued). List of the PD (RLT) tests performed.

Material	Fines content ($< 0.075\text{mm}$) [%]	w_{opt} [% by weight]	G_s [-]	Maximum dry density [gm/cc]	Tests performed with				
					w [% by weight]	S [%]	γ_{dry} [gm/cc]	Stress level	Samples tested
SPV	8.6	6.9	2.68	2.35	2	26.7	2.23	LSL	2
					4	53.5	2.23	LSL	2
					7	78.3	2.16	LSL	1
					7	85.4	2.20	LSL	1
					7	93.6	2.23	LSL	2
					7	99.8	2.26	LSL	1
SG1	3.8	7.5	2.49	2.13	3.5	37.8	2.02	HSL	2
					5.5	59.4	2.02	LSL	1
					5.5	59.4	2.02	HSL	2
					7.5	69.0	1.96	HSL	2
					7.5	74.6	1.99	HSL	2
					7.5	81.0	2.02	HSL	2
					7.5	91.0	2.07	HSL	2
					7.5	98.7	2.09	HSL	2
					8.5	98.6	2.05	HSL	2
					8.5	91.8	2.02	HSL	2
					9.2	99.4	2.02	HSL	2
Siem 25	1.4	5	2.61	2.16	1	10.6	2.10	LSL	2
					3.5	37.2	2.10	LSL	2
					5	53.1	2.10	LSL	2
					7	74.4	2.10	LSL	2
Siem 30	1.2	7.5*	2.61	1.95	3.5	24.0	1.89	LSL	2
					3.5	24.0	1.89	HSL	2

Table 6. List of the static failure triaxial tests performed.

Material	w_{opt} [% by weight]	w for test [% by weight]	Samples tested	Maximum dry density [gm/cc]	Dry density for test [gm/cc]	Static test parameters	
						m [-]	s [kPa]
Skärlunda ($n = 0.62$)	5.5	5.5	1	2.11	2.00	2.03	69.81
Skärlunda ($n = 0.35$)	6.5	1.0	2	2.22	2.15	1.48	256.68
Skärlunda ¹	5.0	3	1	2.08	1.97	1.86	64.65
Hallinden	5.5	3.5	1	2.08	2.01	2.05	60.42
VKB	6.0	4.5	1	2.21	2.19	2.02	52.59
SG1	8.5*	5.5	1	2.13	2.02	1.77	160.91
SG1	8.5*	8.5	1	2.13	2.05	2.62	35.62
Siem 30	7.5*	3.5	1	1.95	1.89	1.85	51.81

Notes:

1. The grain size distribution of this Skärlunda UGM was similar to that of Skärlunda ($n = 0.62$). However, this material was not prepared in the laboratory. Instead, it was taken directly from an HVS test site.

* This w_{opt} value was determined based on the standard Proctor method performed by the Danish Road Directorate. The rest of the w_{opt} values were determined by the modified Proctor method performed by the author.

4.6 Some considerations regarding the test procedure

The RLT tests were carried out in free drainage conditions and the effect of suction and build-up of positive pore water pressure was assumed to be negligible considering the relatively coarse grain size distribution of the UGMs used. The constant confining pressure method was adopted for all the tests since compressed air was used to apply the confining pressure.

The axial deformations of the specimens were measured using three internal LVDTs and the average readings were reported in most of the cases. In some instances, readings from one LVDT were disregarded due to poor measurements. The external LVDT was helpful for the judgement (not reported). Although extreme care was exercised during the installation of the LVDTs, sometimes the anchoring of the LVDTs was not rigid enough for accurate measurements due to the granular nature of the materials, especially for the specimens with (a) coarser grading, (b) lower degree of compaction and (c) higher degree of saturation. Again in some cases, during cyclic loading, rearrangement of the particles caused some rotation of the anchors which tilted the LVDTs and resulted in erroneous measurements. To reduce this rotational effect, fixing the LVDTs using hoops was attempted (Andrei, 2003). However, in this case, it was observed that the movements of the LVDTs affected one another through the hoop, which also affected the reading. Because of this, anchoring the three LVDTs independently was preferred. For improved measurements, other instrumentation techniques such as very light weight local deformation transducers (LDTs) (Araujo and Correia 2009) or laser measurement systems (Marsala et al. 2001) may be better options.

As can be visually observed in Figure 23, the signal-to-noise ratios of the generated signals were pretty good. So, no smoothing was applied during the processing of the raw data. Some scatter in the data was observed, which can be attributed to the granular nature of the materials or poor anchoring or movement of an LVDT during cyclic loading. To account for the variability, usually encountered in RLT tests with UGMs, some of the tests were replicated and the average measurements were reported.

The radial deformation that could be measured using the equipment used for this study was very noisy and not reliable enough to be useful for this research. Hence the radial

deformation was not reported and only the axial deformation was considered given its relatively greater importance.

In this study, the loading sequences from the European standard were applied in consecutive order. It was assumed that this way of loading would take care of the effect of random magnitudes of loading since stress levels for the various stress paths in the different sequences varies from low to high. This can be visualized from Table 2, Table 3 and Figure 21. As a result, going from one sequence to the next, the test specimen experienced somewhat less severe loading in the earlier stage of the current sequence compared to the last few stress paths of the previous sequence. Still, experimenting with applying a random order of the sequences should be considered for future work.

5. RESULTS AND ANALYSES

5.1 Calculations

The raw data generated from the RLT tests were processed using Microsoft Excel. The process was automated by writing Macros with Excel VBA (Visual Basic for Applications). The calculations were performed in the Excel templates in accordance with the European Standard (CEN 2004a).

5.2 Calibration of the models

The models used in this study were calibrated using the RLT test data employing the least square curve fitting procedure (Gujarati and Porter 2009, Johnson et al. 2011). First, the parameters of the models were assumed based on the literature and some engineering judgement. Each model with the assumed parameters was then used to predict the outcome based on a set of values of the relevant input variables. The error in prediction, which is the difference between the actual measured value and the predicted value by the model, was calculated for each data point. The sum of the errors squared for all the data points for a particular test was calculated, which was then minimized by optimizing the parameters of the models. The Solver add-on in Microsoft Excel was used for the optimizations which minimized the sum of the square of errors by adjusting the parameters. It should be noted that the final optimized values of the parameters were dependent on the initial estimated values. There may be several combinations of the values of the parameters that will produce acceptable quality of fit for a model. When a model has a larger number of regression (material) parameters, there may be greater numbers of combinations of the values of the parameters to achieve reasonable quality of prediction. Thus care should be taken during the initial estimations. In this study, the parameters were restricted to positive values. However, further restrictions on the parameters may need to be applied to prevent obtaining unrealistic values. Again, optimized parameters of a model should be verified by employing the model in different test conditions. Based on further research and experience, reasonable ranges for the values of the parameters need to be established.

5.3 Statistical evaluation of the quality of fit

To determine how well a model fits the measured values in an RLT test, goodness of fit statistics were used. In the papers the following different types of measures were used (Gujarati and Porter 2009):

The coefficient of determination, R^2 defined as:

$$R^2 = 1 - \frac{SS_{res}}{SS_{tot}} \quad (10)$$

where $SS_{tot} = \sum_i (y_i - \bar{y})^2$ is the total sum of squares, $SS_{res} = \sum_i (y_i - f_i)^2$ is the residual sum of squares, $\bar{y} = \frac{1}{n_d} \sum_{i=1}^{n_d} y_i$ is the mean of the measured data and n_d is the number of data points. y_i is a measured data point and f_i is the corresponding prediction by a model. An R^2 of 1 indicates that the model perfectly fits the measured data. Using this definition of R^2 , it can be observed that R^2 can never be greater than one, but it is possible to get negative values.

The adjusted coefficient of determination, *adjusted* R^2 defined as:

$$adjustedR^2 = 1 - \frac{SS_{res}(n_d - 1)}{SS_{tot}(n_d - p_m - 1)} \quad (11)$$

where p_m is the number of regression parameters in a model. This measures the quality of fit of a model considering the number of parameters in the model, thus allowing for a fair comparison of the models. The adjusted R^2 can be negative. Its value is either less than or equal to that of R^2 .

The root mean square error (*RMSE*), defined as:

$$RMSE = \sqrt{\frac{SS_{res}}{n_d}} \quad (12)$$

This simply measures the differences between the values predicted by a model and the values actually observed. Thus the lower the *RMSE*, the better is the quality of fit for a model.

5.4 Shakedown range calculation

For the MS RLT tests, the shakedown ranges occurring in a UGM during the application of the different stress paths were calculated using the criteria given by Equation 5. These were calculated both for the measured data and the predictions by the different models. The shakedown range predicted by a model was then compared to that observed. An example of this is presented in Table 7 for the test applying the LSL on Siem 30 with $w = 3.5\%$. The shaded cells in the table highlight the wrong predictions of the shakedown ranges. The accuracies of the predictions were calculated based on the number of the shakedown ranges predicted correctly by the models.

Table 7. An example of the shakedown range predictions by the models (Siem 30, $w = 3.5\%$, LSL).

Stress path no.	Confining stress/ Deviator stress (kPa/kPa) (LSL)	Shakedown ranges				
		Test data	Tseng and Lytton	Gidel et al.	Korkiala- Tanttu	Modified Korkiala- Tanttu
1	20/20	B	C	B	B	B
2	20/40	B	C	B	B	B
3	20/60	B	C	B	C	C
4	20/80	B	C	C	C	C
5	20/100	B	C	C	C	C
6	20/120	C	C	C	C	C
7	45/60	A	A	A	A	A
8	45/90	A	B	A	A	A
9	45/120	A	B	A	A	A
10	45/150	B	B	A	B	B
11	45/180	B	B	C	B	B
12	45/210	B	B	C	C	C
13	70/80	A	A	A	A	A
14	70/120	A	A	A	A	A
15	70/160	A	B	A	A	A
16	70/200	A	B	A	A	A
17	70/240	B	B	A	B	B
18	70/280	B	B	C	B	B
19	100/100	A	A	A	A	A
20	100/150	B	A	A	A	A
21	100/200	B	A	A	A	A
22	100/250	B	B	A	A	A
23	100/300	B	B	A	A	A
24	100/350	B	B	B	B	B
25	150/100	A	A	A	A	A
26	150/200	A	A	A	A	A
27	150/300	A	A	A	A	A
28	150/400	B	B	A	A	A
29	150/500	B	B	B	B	B
30	150/600	C	B	C	C	C
Accuracy (%)			60	60	70	70

6. SUMMARY OF THE APPENDED PAPERS

This thesis is based on five interrelated papers relevant to the deformation behaviour of UGMs. The first paper deals with the influence of moisture on the RD behaviour of UGMs. The second and third papers are about modelling the PD behaviour of UGMs under MS cyclic loading. In the fourth and fifth papers a new model has been proposed for the PD behaviour of UGMs and the impact of moisture was specifically investigated. These papers are enclosed at the end of this thesis and are briefly described in the following sub-sections.

6.1 Paper I: Moisture Influence on the RD Behaviour of UGMs

The objective of this study was to investigate the influence of moisture on the RD behaviour of UGMs. The impact of moisture was compared in two cases: (a) when the deformation is mostly resilient with very low accumulated PD and (b) when the RD is accompanied by significant amount of accumulated PD. The aim was to enhance the understanding and to improve the modelling of the impact of moisture on the RD properties of UGMs. The sensitivity to moisture of the various grain size distributions of UGMs was also investigated.

The study was carried out using six UGMs. These were three different grain size distributions of Skärlanda, SPV, VKB and SG1. RLT tests were carried out on these materials following the procedure for the RD tests from the European standard to investigate case (a). According to this test procedure, several stress paths were applied to the test specimen with 100 load cycles for each stress path. The accumulated PD in this case was very low and the deformation of the material was mostly resilient. To investigate case (b), the MS RLT test for the PD behaviour of UGMs from the European standard was used for identical specimens used for case (a). In this case, several stress paths were applied to the test specimen with 10,000 load cycles for each stress path. This resulted in a significant amount of accumulated PD. All the materials were tested for a series of moisture contents.

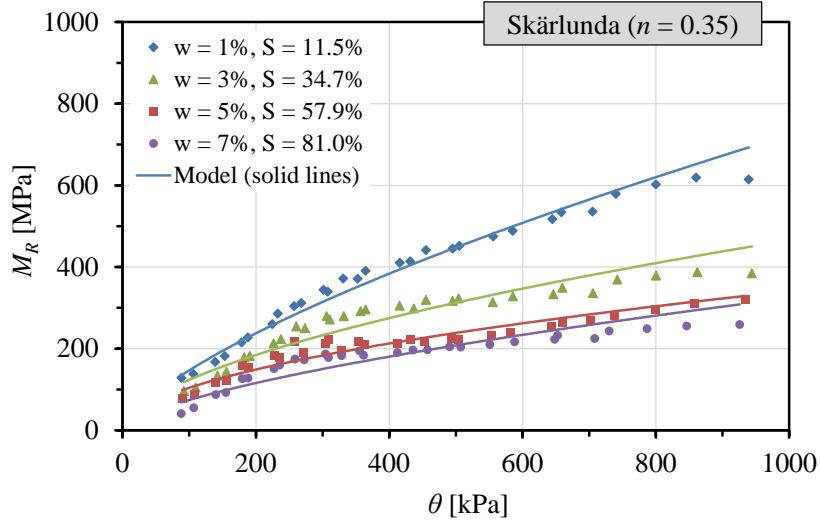
Results from the RD tests for case (a) showed that M_R decreased with increased moisture content, as shown in Figure 26. The k - θ model was calibrated for the tests and the influence of moisture on the parameters k_1 and k_2 was investigated. k_1 was found to decrease with increasing moisture while k_2 remained unaffected, as shown in Figure 27. Based on these results, k_1 was expressed as the following exponential function of S :

$$k_1 = a_1 e^{-a_2 S} \quad (13)$$

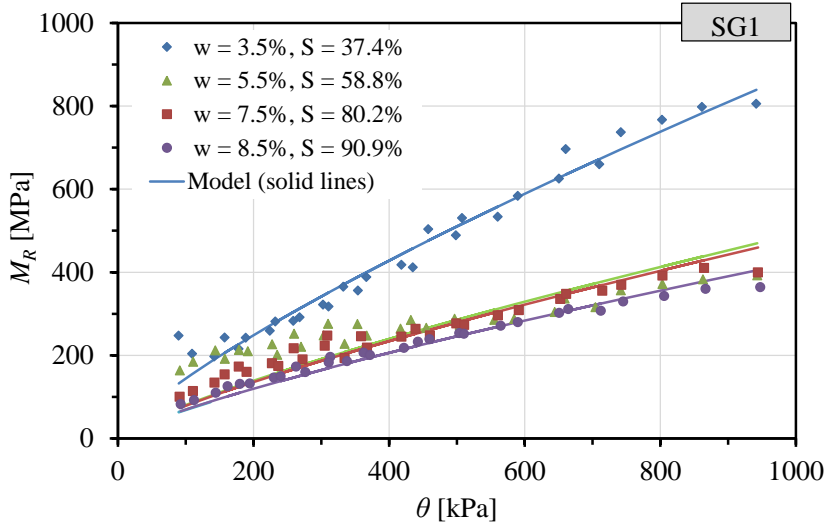
where a_1 and a_2 are material parameters. Thus the k - θ model was expressed, including S as a predictive variable, as:

$$M_R = a_1 e^{-a_2 S} p_a \left(\frac{\theta}{p_a} \right)^{k_2} \quad (14)$$

This expression, as well as, the MEPDG M_R -moisture model (Equation (4)) was used to model the results obtained here, shown in Figure 28. Both of these models worked pretty well in this case. The tests on the three grain size distributions of the Skärlanda UGMs showed that the moisture sensitivity increased with an increasing amount of fines.

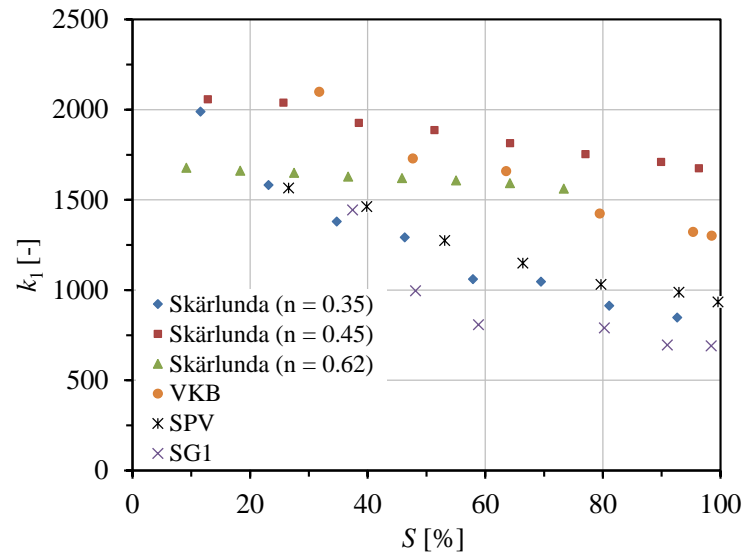


(a)

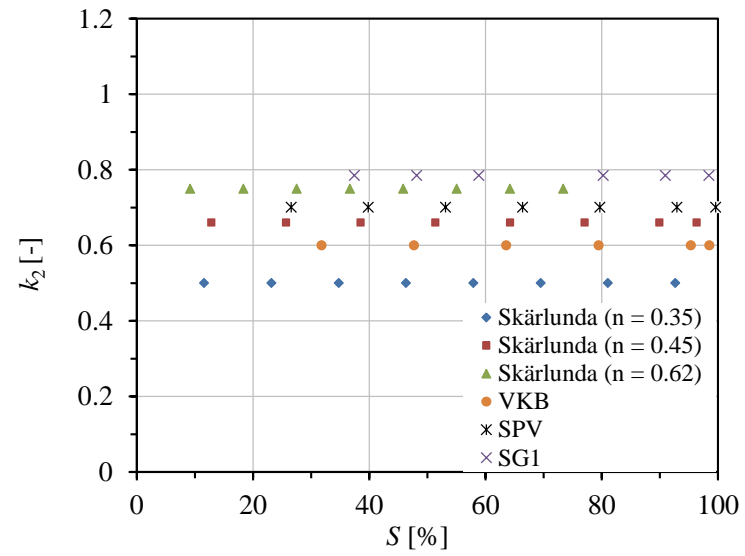


(b)

Figure 26. M_R as a function of θ for various w and S from the RD tests: (a) Skärlanda ($n = 0.35$), (b) SG1.



(a)



(b)

Figure 27. The parameters k_1 and k_2 as a function of S from the RD tests.

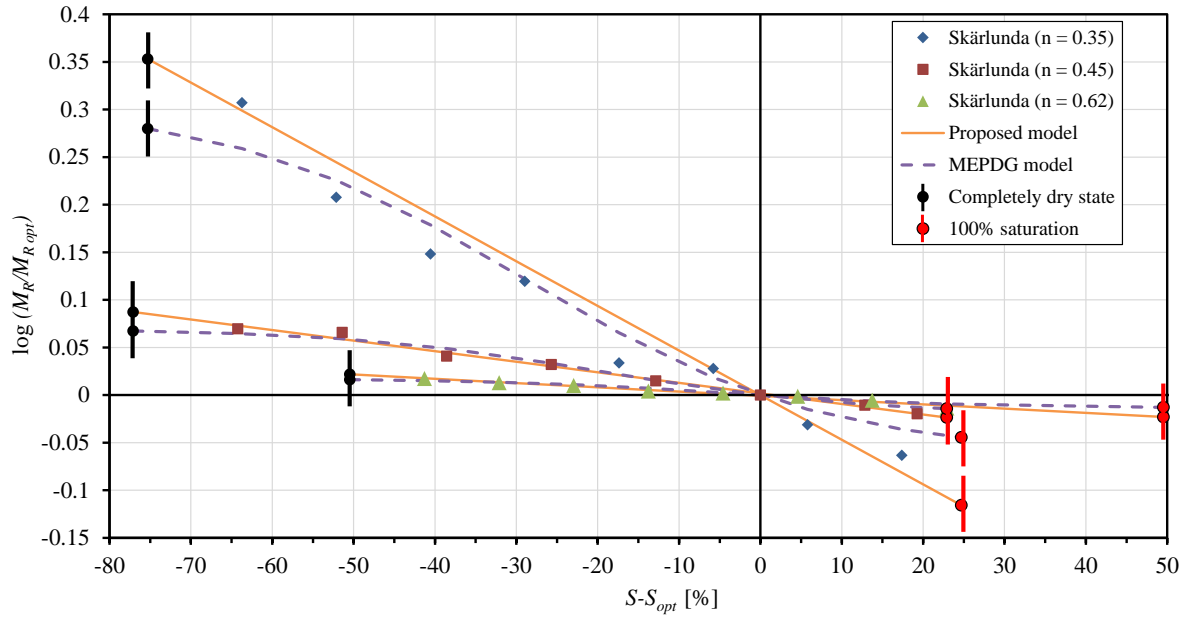
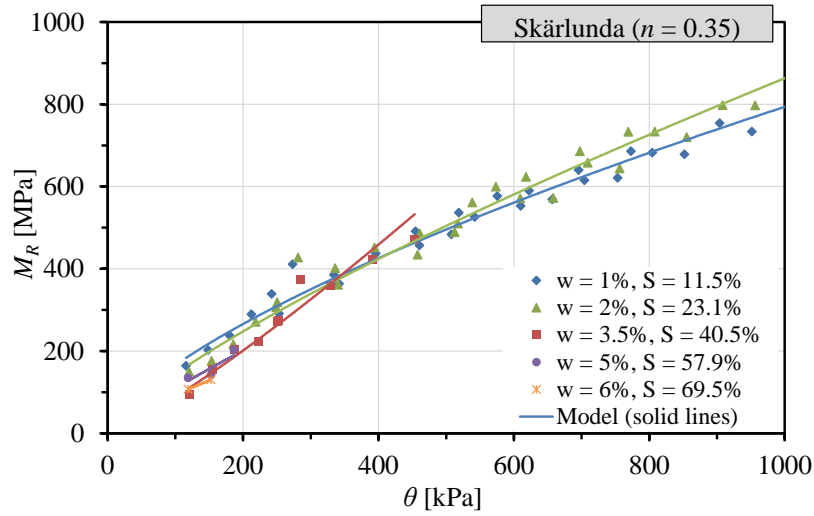
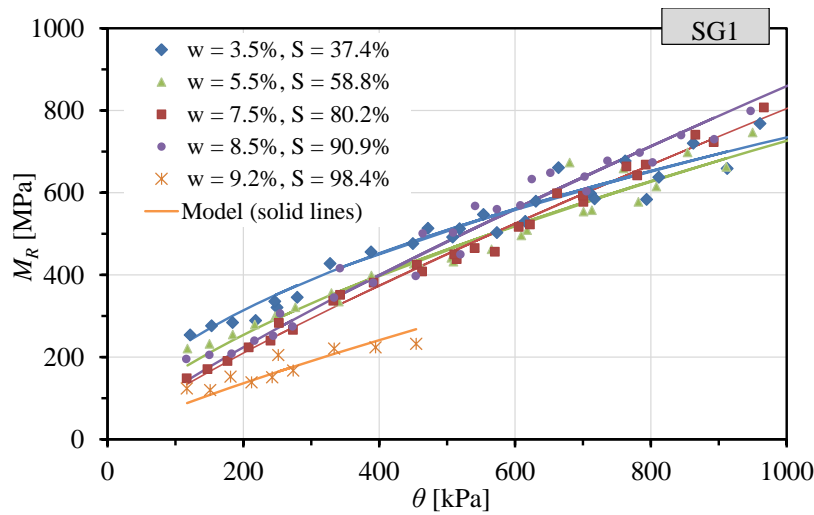


Figure 28. Normalized M_R as a function of change in S (for $\theta = 550$ kPa): Modelled vs. measured.

The results from the PD tests, for case (b), showed that at the earlier stages of the tests, moisture decreased the M_R of the UGMs. At the later stages, corresponding to the higher θ values, for relatively large N when PD is large, M_R increased with increased moisture, usually up to the w_{opt} . This effect is visible in Figure 29 where the M_R vs θ curves for the different w 's are crossing each other. Above the w_{opt} , M_R always decreased. For this case, the parameter k_1 of the k - θ model decreased with increased moisture while the parameter k_2 increased with moisture, as shown in Figure 30. These results could not be modelled using the MEPDG M_R -moisture model. Although it was not explored in this study, it may be possible to implement the proposed model, expressed in Equation (14), if k_2 is expressed as a function of moisture.

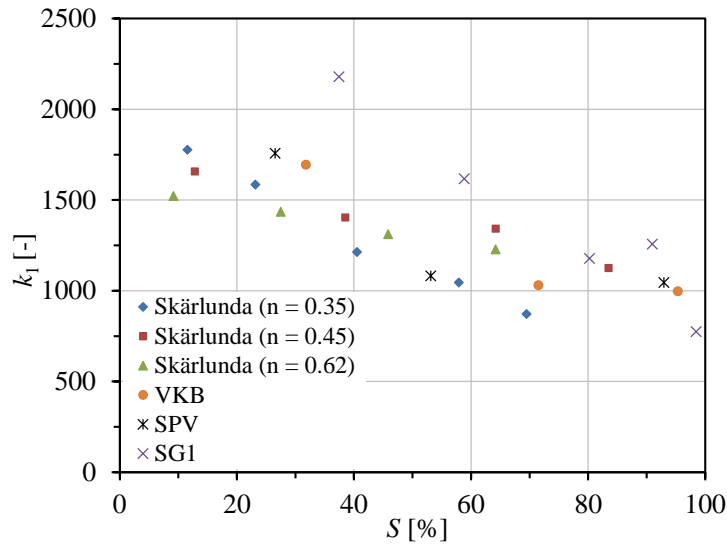


(a)

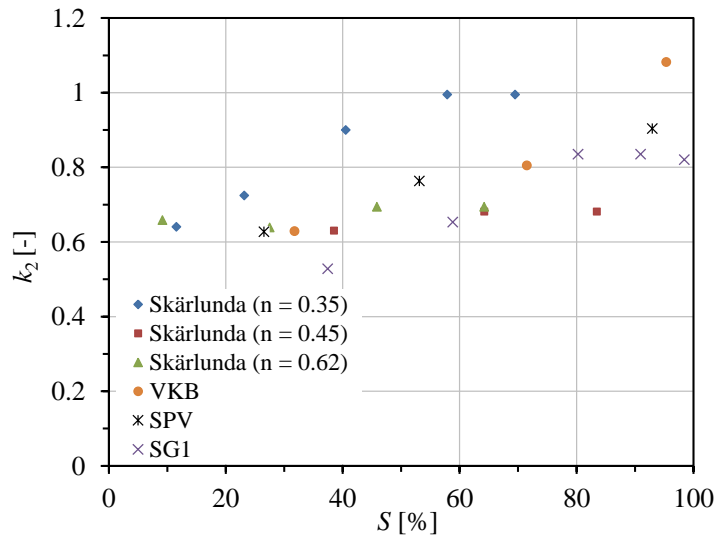


(b)

Figure 29. M_R as a function of θ for various w and S from the PD tests: (a) Skarlunda ($n = 0.35$) (b) SG1.



(a)

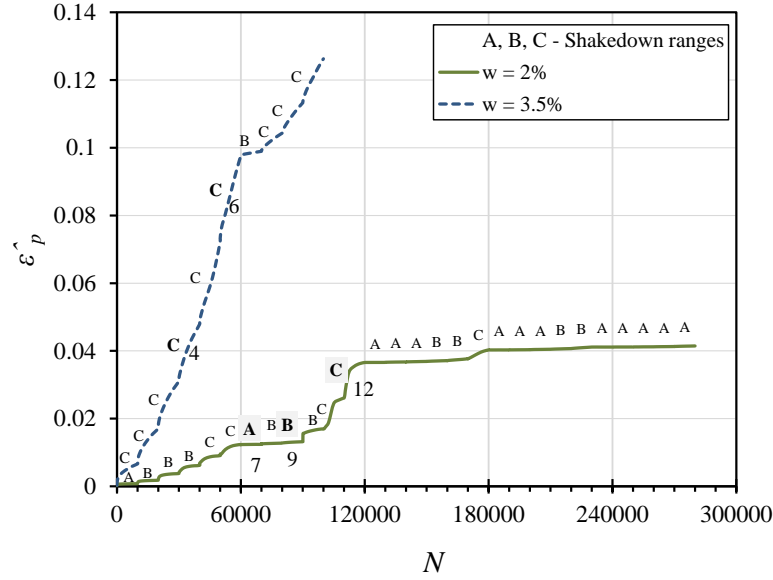


(b)

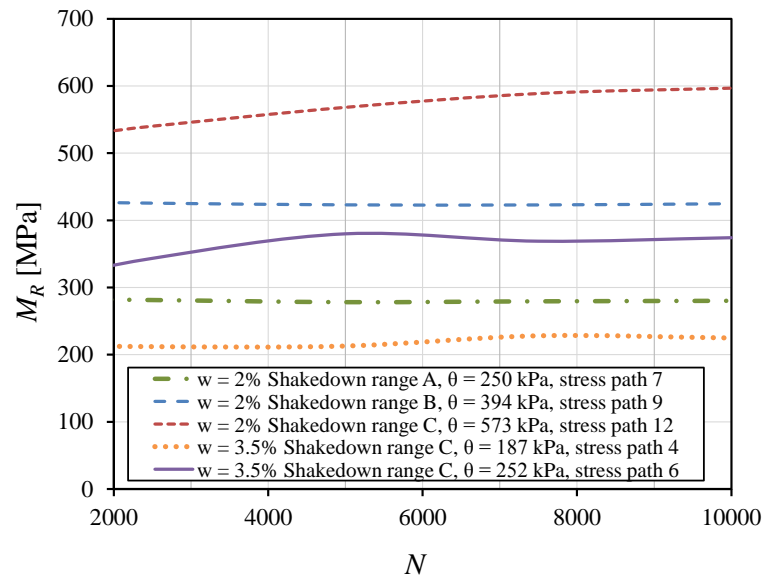
Figure 30. The parameters k_1 and k_2 as a function of S from the PD tests.

The results from the PD tests were further analyzed by plotting the accumulated permanent strain ($\hat{\varepsilon}_p$) against N including the shakedown ranges of the different stress paths and plotting M_R as a function of N , as shown in Figure 31. It was observed that M_R increased with N when the shakedown range was C. In shakedown range A and B, M_R was fairly unchanged. Since for the tests with a higher w the number of stress paths with shakedown range C was higher, it was thought that the specimens with a higher w experienced a relatively rapid increase of M_R with N that resulted in the higher M_R during the later stages of the tests. It was further explained that moisture aided the PC, reorientation and change in packing arrangement of the particles which in turn increased the M_R of the material

(Yideti et al. 2013b, Liu et al. 2014). Thus when w was increasing up to w_{opt} , the material experienced a faster PC aided by moisture that resulted in increased M_R . This led to the steeper M_R versus θ curves for the specimens with a higher w .



(a)



(b)

Figure 31. Evolution of M_R with N and PD for different shakedown ranges (for Skärlanda ($n = 0.35$), $w = 2\%$ and 3.5% , PD test with HSL).

The effect of accumulated PD on M_R was further investigated by plotting the M_R of the same material obtained from the RD test, the PD tests with the LSL and the HSL, shown in Figure 32. It was found that the PD test with the HSL resulted in the highest $\hat{\epsilon}_p$ and the

highest M_R at the later stage of the test. At the earlier stages (low $\hat{\varepsilon}_p$) of the tests, the M_R values were pretty similar for all the tests. This increase in M_R with increased PD was thought to be due to PC. Hence this study suggested that the impact of PD due to PC should be considered for better modelling of the impact of moisture on M_R .

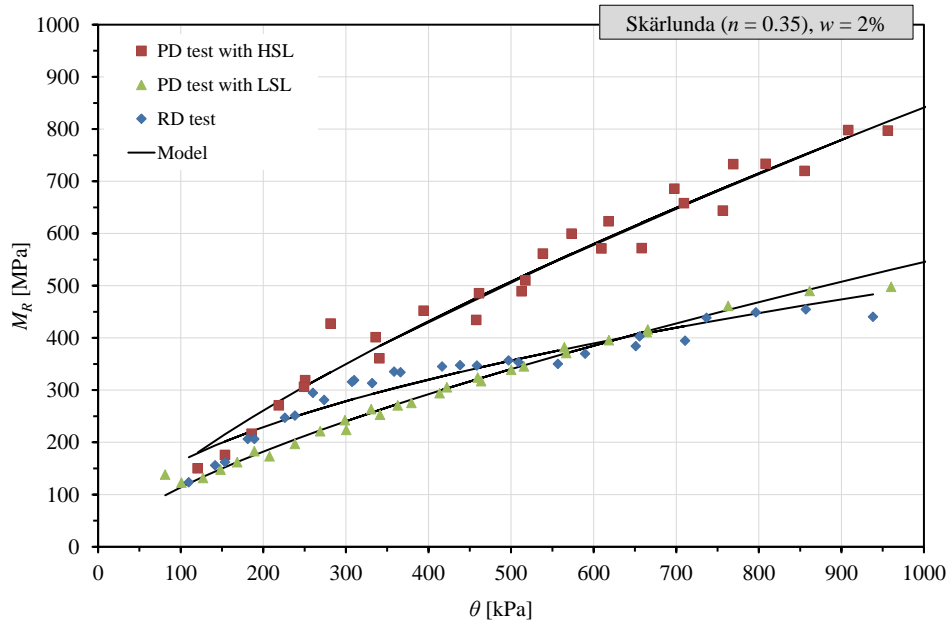


Figure 32. Comparison of the M_R values from the RD test and the PD tests with the HSL and the LSL for Skärlunda ($n = 0.35$) with $w = 2\%$.

6.2 Paper II: Evaluation of PD Characteristics of UGMs by Means of MS RLT tests

This paper deals with the modelling of the accumulation of PD in UGMs under MS cyclic loading. As discussed in section 3.2.1, the MS RLT test is a more convenient way for a comprehensive study of the PD behaviour taking into account the effect of variable stress levels and stress history. Since the PD models cannot be directly applied to the MS loading conditions, a general formulation based on the time hardening concept (Lytton et al. 1993) was introduced in this paper. With this formulation, the PD models can be extended to apply for the MS RLT tests. The procedure is described in the following paragraph.

Applying the time hardening concept, shown in Figure 33, at the beginning of any level (i) of the MS RLT test, the accumulated permanent strain from the previous loading stages is used to calculate the equivalent number load cycles (N_i^{eq}) required to attain the same amount of strain for the current stress level alone. This N_i^{eq} is then used to modify the total number of load cycles, N from the beginning of the test to get the effective number of load cycles as ($N - N_{i-1} + N_i^{eq}$), where N_{i-1} is the total number of load cycles at the end of ($i-1$)th stress path. Thus this effective number of load cycles is used to calculate any further accumulation of permanent strain during the current loading stage. If the stress level during the current loading stage is significantly lower than the previously occurring stress levels, the calculated N_i^{eq} approaches infinity and it is assumed that no further permanent strain will occur during this stage. Hence, using this procedure, it is possible to model the entire range of the MS RLT test continuously.

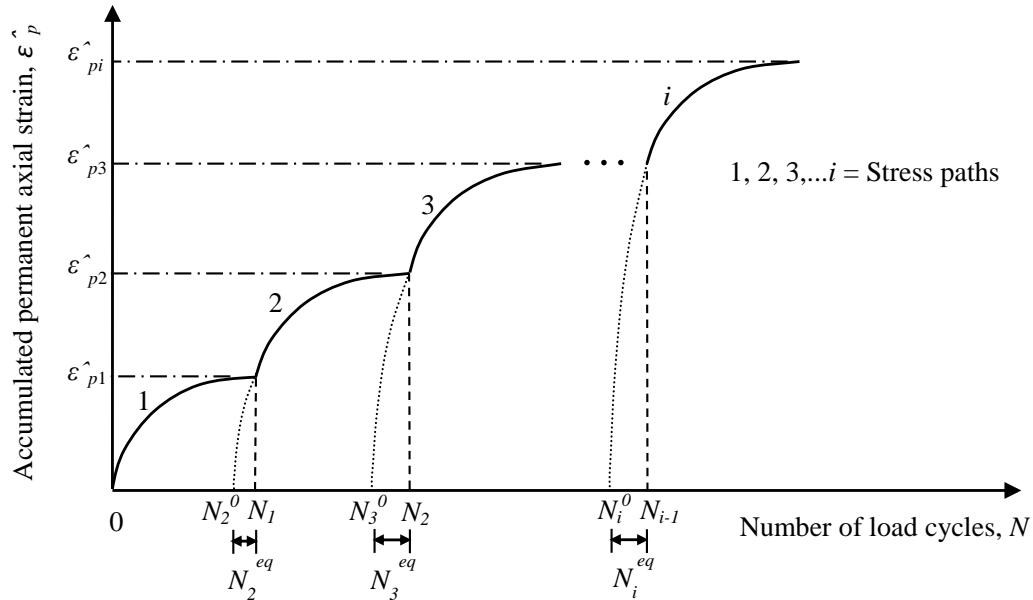


Figure 33. Demonstration of the time hardening approach.

The PD models that describe the accumulation of PD as a function of N and stress level can be generalized for a single stress path in an RLT test as:

$$\hat{\varepsilon}_p(N) = f_1(N)f_2(p, q, \varepsilon_r) \quad (15)$$

For MS RLT test, applying the time hardening formulation, this can be expressed as:

$$\hat{\varepsilon}_{p_i}(N) = f_1(N - N_{i-1} + N_i^{eq})f_2(p_i, q_i, \varepsilon_{r_i}) \quad (16)$$

where the suffix i refers to the i^{th} stress path. N_i^{eq} is calculated as:

$$N_i^{eq} = f_3(\hat{\varepsilon}_{p_{i-1}}, p_i, q_i, \varepsilon_{r_i}) \quad (17)$$

where $\hat{\varepsilon}_{p_{i-1}}$ is the accumulated permanent strain at the end of $(i-1)^{\text{th}}$ stress path.

To validate this formulation, some existing models were extended for MS loading conditions and were applied for MS RLT tests. Thus, using this approach, the model proposed by Korkiala-Tanttu (2005) was expressed for MS RLT tests as:

$$\hat{\varepsilon}_{p_i}(N) = C(N - N_{i-1} + N_i^{eq})^b \frac{R_i}{A - R_i} \quad (18)$$

where

$$N_i^{eq} = \left[\frac{\hat{\varepsilon}_{p_{i-1}}(A - R_i)}{CR_i} \right]^{\frac{1}{b}} \quad (19)$$

This model was also slightly modified for MS RLT test conditions as:

$$\hat{\varepsilon}_{p_i}(N) = C(N - N_{i-1} + N_i^{eq})^{c(R_i)^d} \frac{R_i}{A - R_i} \quad (20)$$

where c and d are material parameters and

$$N_i^{eq} = \left[\frac{\hat{\varepsilon}_{p_{i-1}}(A - R_i)}{CR_i} \right]^{c^{-1}(R_i)^{-d}} \quad (21)$$

The model proposed by Gidel et al. (2001) was extended as:

$$\hat{\varepsilon}_{p_i}(N) = \varepsilon^0 \left[1 - \left(\frac{N - N_{i-1} + N_i^{eq}}{100} \right)^{-B} \right] \left(\frac{L_{\max,i}}{p_a} \right)^u \left(m + \frac{s}{p_{\max,i}} - \frac{q_{\max,i}}{p_{\max,i}} \right)^{-1} \quad (22)$$

where

$$N_i^{eq} = 100 \left(1 - \frac{\hat{\varepsilon}_{p_{i-1}}}{\varepsilon_0} \left(\frac{L_{\max,i}}{p_a} \right)^{-u} \left(m + \frac{s}{p_{\max,i}} - \frac{q_{\max,i}}{p_{\max,i}} \right)^{-1} \right)^{-1/B} \quad (23)$$

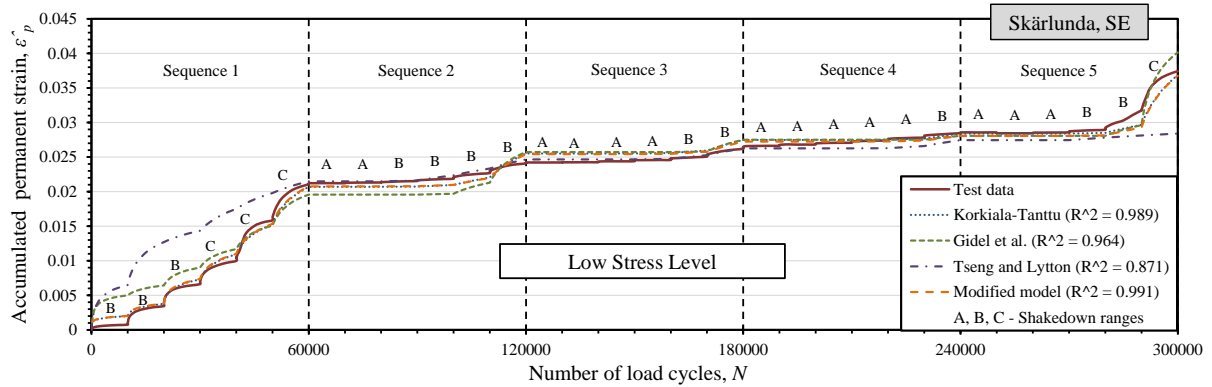
And the model proposed by Tseng and Lytton (1989) was extended as:

$$\hat{\varepsilon}_{p_i}(N) = \varepsilon_{r_i} \varepsilon_0 e^{-\left(\frac{\rho}{N - N_{i-1} + N_i^{eq}}\right)^\beta} \quad (24)$$

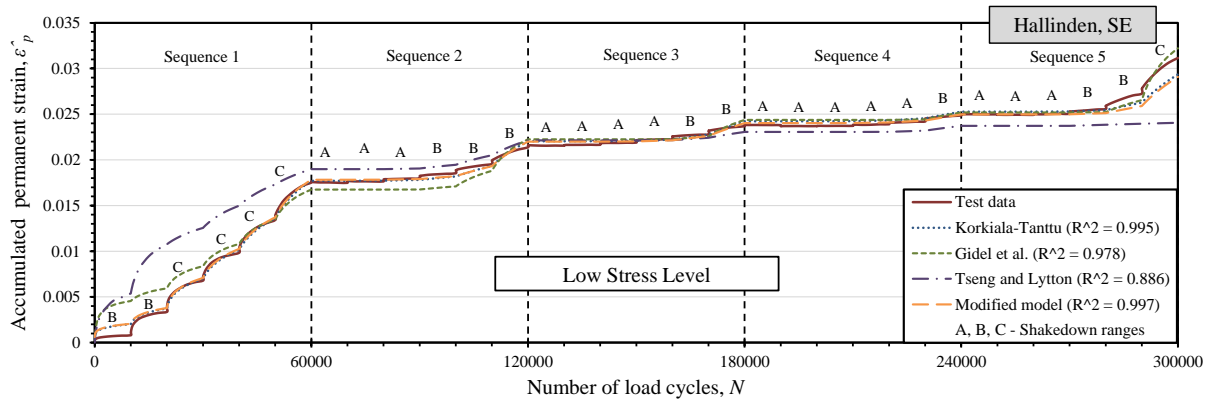
where

$$N_i^{eq} = \rho \left(-\ln \left(\frac{\hat{\varepsilon}_{p_{i-1}}}{\varepsilon_{r_i} \varepsilon_0} \right) \right)^{-1/\beta} \quad (25)$$

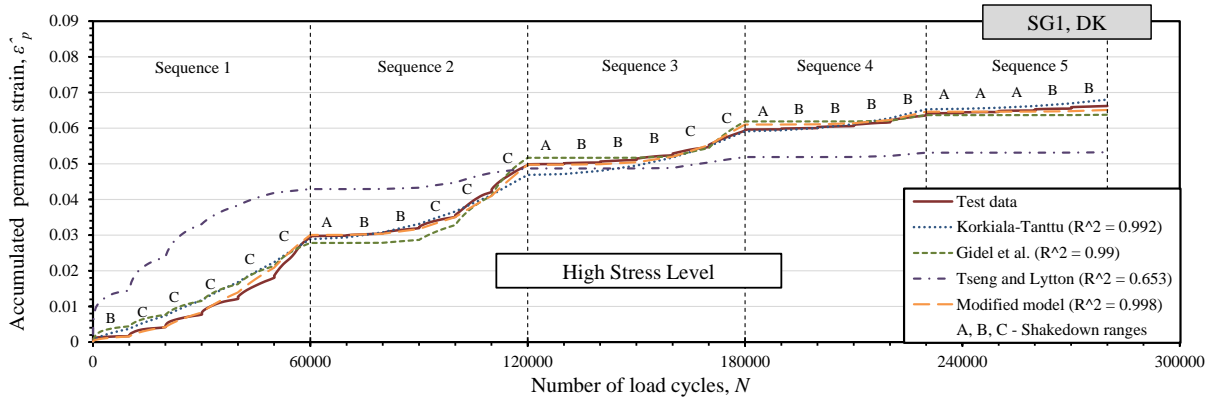
These extended models were calibrated using data from MS RLT tests on several typical UGMs. The least square curve fitting method was used for the calibrations. The qualities of fit achieved with the individual models were evaluated using the goodness of fit statistics. Additionally, the shakedown ranges occurring for all the stress paths in the MS RLT tests were calculated and the predictions using the models were compared. The measured and modelled accumulation of permanent strain for the tests carried out here has been presented in Figure 34. This shows that it is possible to model the PD behaviour of UGMs in MS loading conditions applying the time hardening formulation with some good qualities of fits. In fact, this formulation is material independent and simply applied to a model. Thus the quality of fit that can be achieved is dependent on the model used. Among the models used in this study, the modified version of the Korkiala-Tanttu model performed better than the other models.



(a)



(b)



(c)

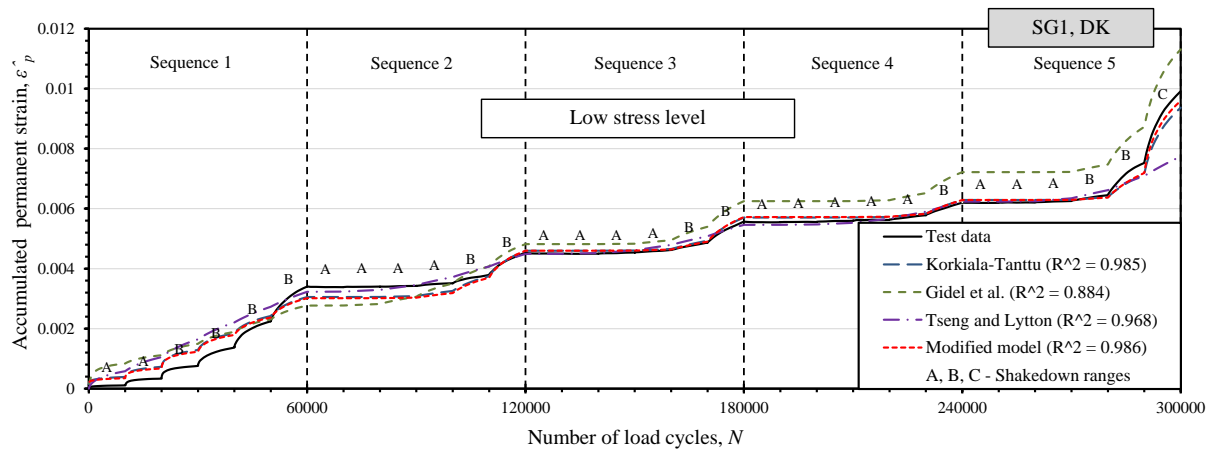
Figure 34. Accumulation of permanent strain: Test data and the calibrated models.

6.3 Paper III: Predicting PD Behaviour of UGMs

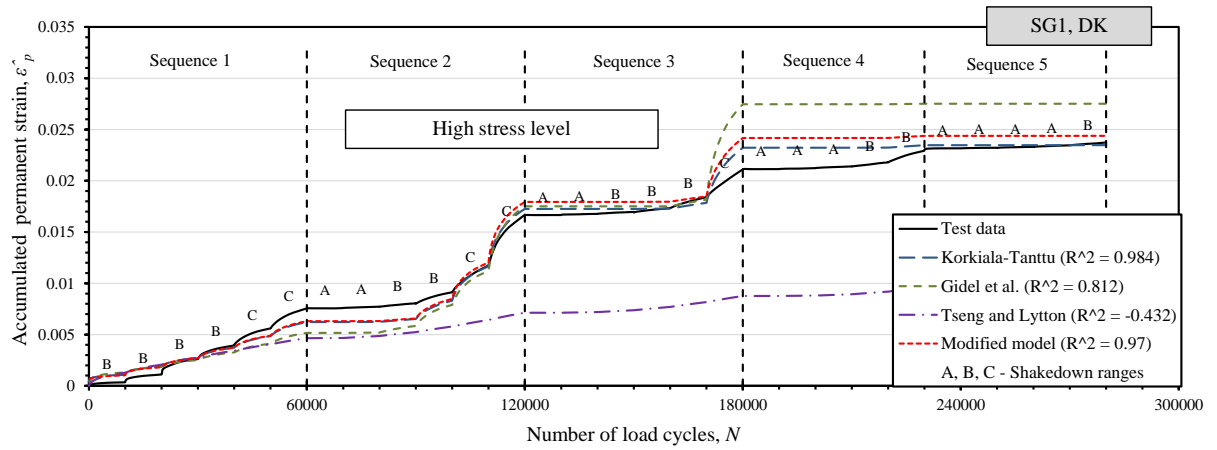
This paper is a continuation of Paper II. Here, the time hardening formulation was extensively applied for more tests. The objective was to test the validity of the models by applying them to predict the PD behaviour in a different set of stress levels other than those used for their calibration. In this case, the MS RLT tests were carried out on identical specimens using both LSL and HSL. The data with one set of loading were used to calibrate the models and the models were then used to predict the PD behaviour for the tests with the other set of stress levels. The performance of these models was evaluated and compared. For most of the cases the model proposed by Korkiala-Tanttu performed better than the other models.

The MS RLT tests were carried out using five different materials. An example of the predictions by the different models in a calibration test using LSL for a Danish UGM, referred to here as SG1, is shown in Figure 35 (a). The predictions by these models calibrated for SG1, for the test using HSL, are shown in Figure 35 (b). This showed that the models performed pretty well in predicting the PD behaviour for two different stress situations. In addition to the paper, an example of predicted versus measured plots for a Swedish UGM, referred to here as VKB, SE is presented in Figure 36.

The quality of fit, expressed using the adjusted coefficient of determination (R^2), achieved using the different models for all the tests on the different models is presented in Figure 37. The comparisons of the models in terms of correct predictions of the shakedown ranges for all the stress paths in the MS RLT tests are given in Figure 38.

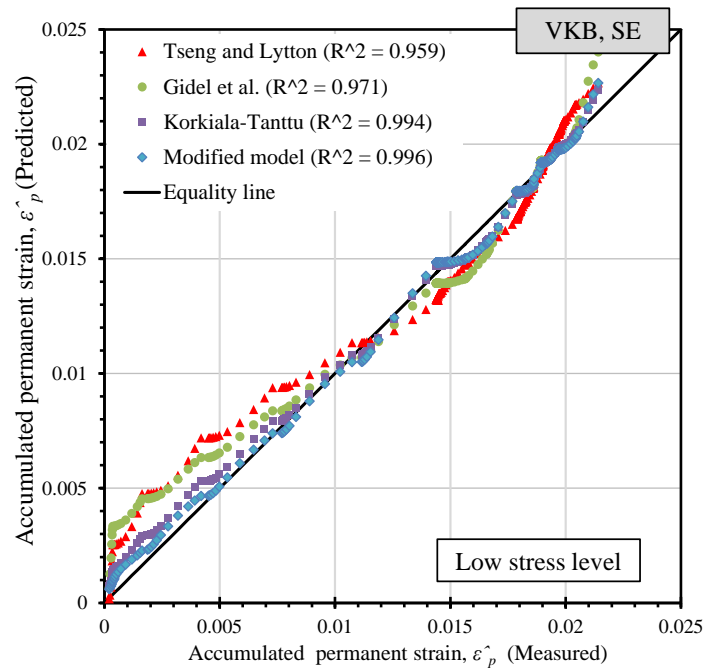


(a)

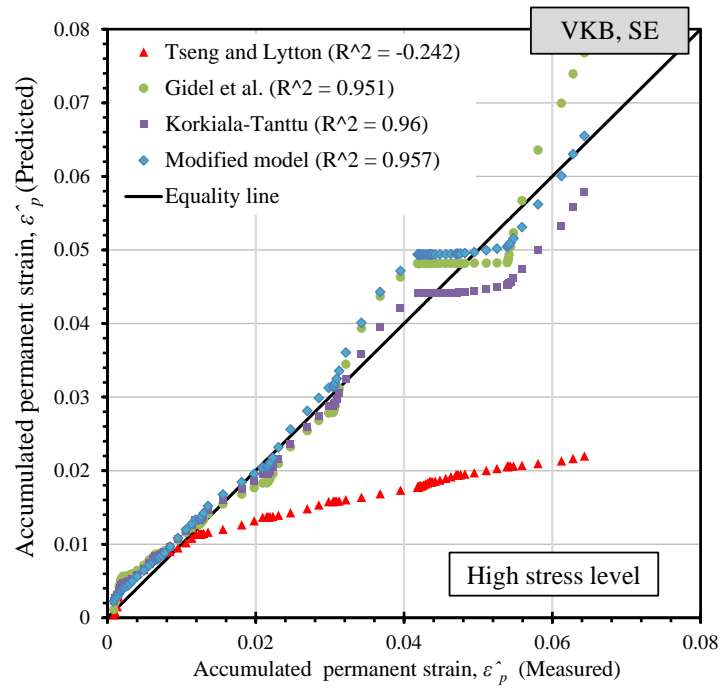


(b)

Figure 35. Accumulation of permanent strain: Test data and the calibrated models: (a) for the calibration test and (b) for the validation test.



(a)



(b)

Figure 36. Accumulated permanent strain: Predicted versus measured plots (a) for the calibration test and (b) for the validation test.

6. Summary of the Appended Papers

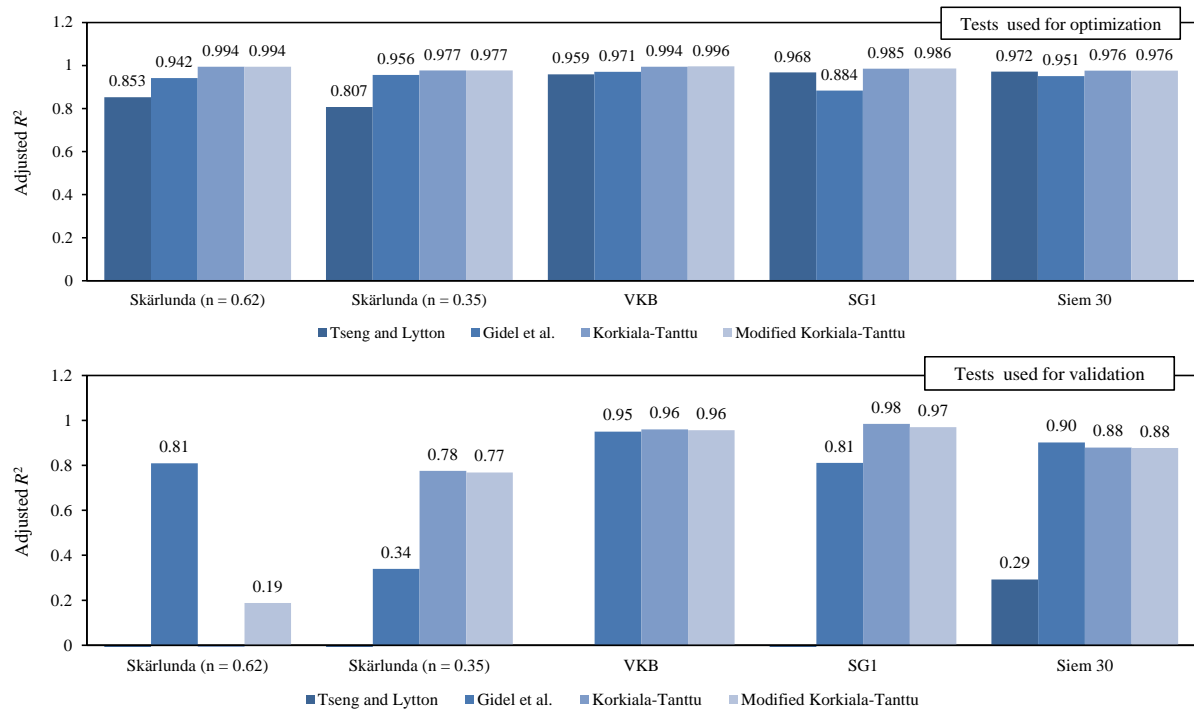


Figure 37. Comparison of the quality of fit (adjusted R^2 values).

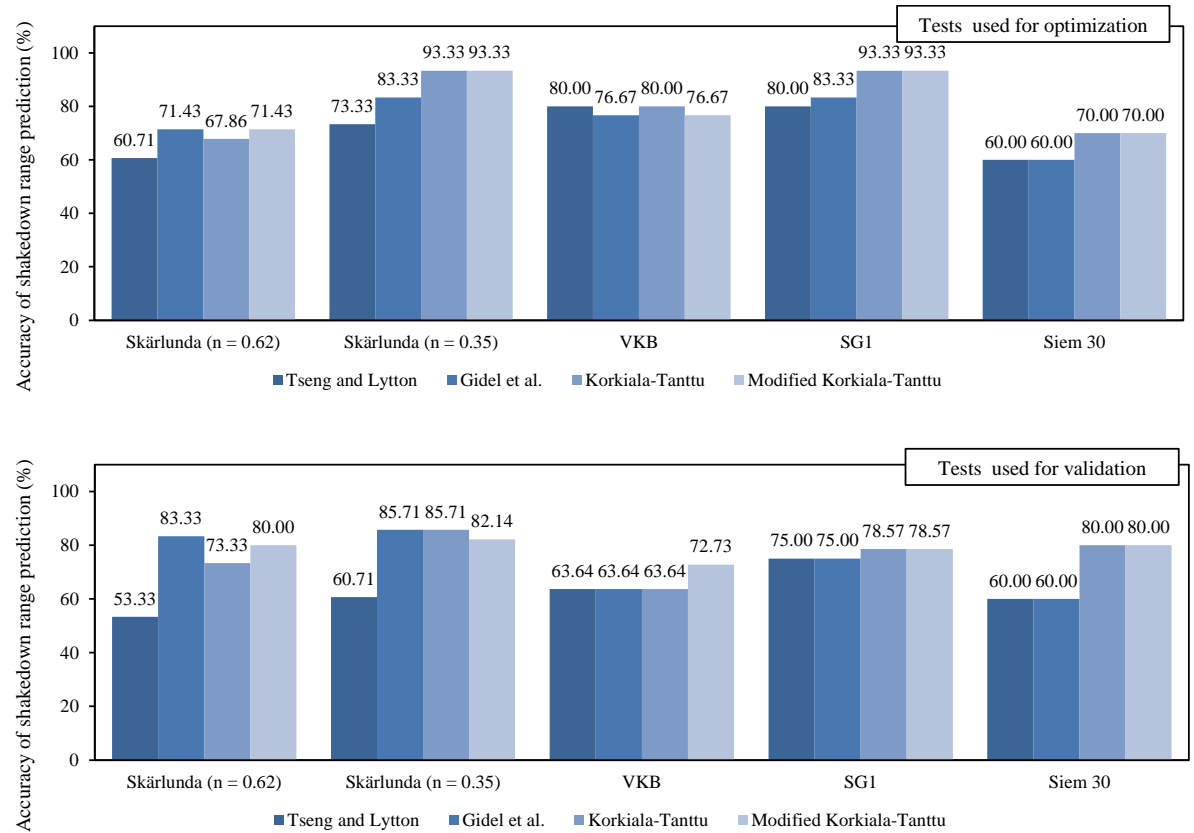


Figure 38. Accuracy of the shakedown range predictions [%].

This study showed that it is possible to predict the PD behaviour of UGMs in MS RLT tests using the existing models with reasonable accuracy when the time hardening approach is applied. The accuracy in prediction is dependent on the model used. Generally the modified version of the Korkiala-Tanttu model was found to be a better performer. In contrast, the model by Tseng and Lytton did not perform very well, especially in the tests for validation of the models. One possible explanation may be that the model expresses the effect of stress level through ε_r . However, ε_r is not constant throughout the application of a specific stress path. It stabilizes after a certain number of load applications which are used to calculate the M_R . To predict PD using this model, ε_r needs to be calculated using M_R which, in turn was predicted for the different stress conditions using the $k-\theta$ model. Thus the error in predicting the M_R using the $k-\theta$ model was translated to the prediction of the PD which amplified the total error in predictions. Again, the M_R of a UGM, at a specific stress condition, determined using LSL versus HSL needs to be investigated because of the different degree of post-compaction involved. Hence the model may not be suitable for MS loading conditions. Generally, all of these models, when calibrated using MS RLT tests, may need further modifications to predict the actual behaviour of the materials in a pavement structure.

6.4 Paper IV: Characterizing the Impact of Moisture on the PD Behaviour of UGMs

In this paper studies have been carried out to characterize the impact of moisture on the PD behaviour of UGMs. MS RLT tests were performed on several UGMs with a range of moisture contents. The sensitivity to moisture for different grain size distribution was also examined. Since the models that performed well in the previous studies (Papers II and III) require separate static failure triaxial tests besides the RLT tests for their calibration, an alternative model was developed to reduce this effort. The aim was also to reduce the number of material parameters.

The following model was developed based on the MS RLT tests:

$$\hat{\varepsilon}_p(N) = aN^{bS_f} S_f \quad (26)$$

where a and b are regression parameters related to the material. The term S_f describes the effect of stress condition on the development of PD which is expressed as:

$$S_f = \frac{\left(\frac{q}{p_a}\right)}{\left(\frac{p}{p_a}\right)^\alpha} \quad (27)$$

where q is the deviator stress, p is the hydrostatic stress (one-third of the sum of the principal stresses) and α is a parameter determined using regression analysis. The term $p_a = 100$ kPa (reference stress taken equal to the atmospheric pressure) was used to make the expression non-dimensional. It should be noted here that the term S_f in Equation (26) and Equation (27) was originally used as S in Paper IV which was later changed to S_f in Paper V to differentiate it from the degree of saturation (S) used in Paper I.

The proposed model can be calibrated using a single MS RLT test with satisfactory performance. Thus it was possible to evaluate the parameters of this model for the RLT tests with a series of moisture contents with minimal effort. Then the sensitivity of the parameters of the model to moisture was analysed.

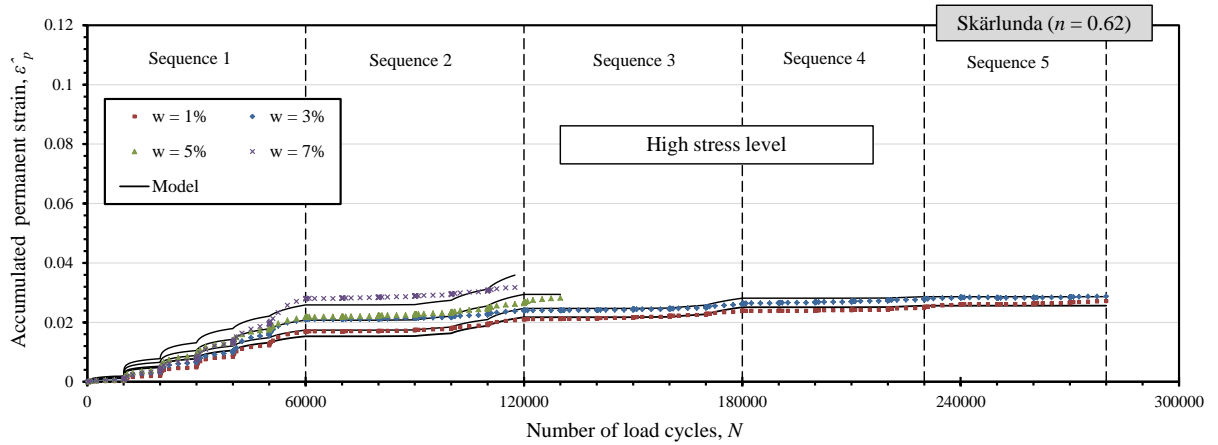
The model was used for MS RLT tests applying the time hardening concept, as in Papers II and III, as:

$$\hat{\varepsilon}_{p_i}(N) = a(N - N_{i-1} + N_i^{eq})^{b(S_f)_i} (S_f)_i \quad (28)$$

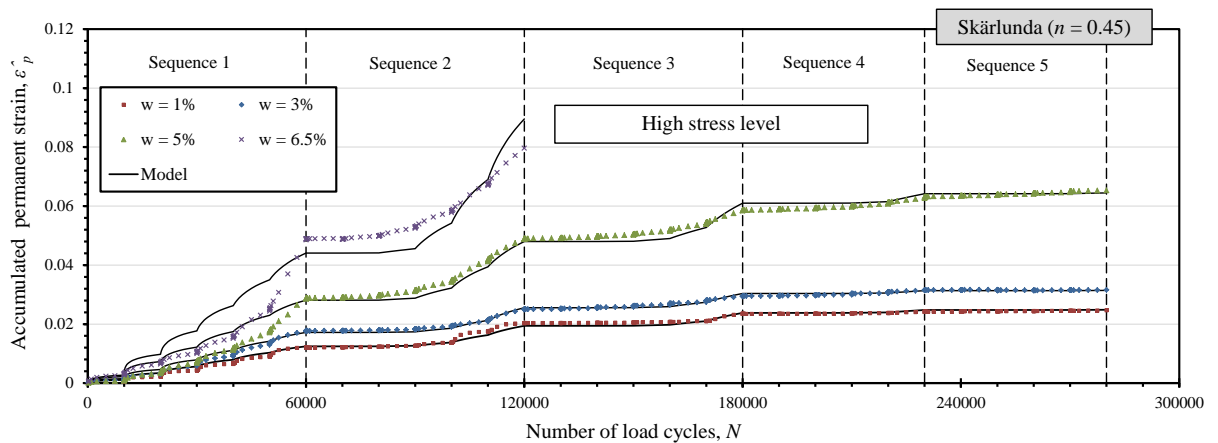
where

$$N_i^{eq} = \left[\frac{\hat{\epsilon}_{p_{i-1}}}{a(S_f)_i} \right]^{b^{-1}(S_f)_i^{-1}} \quad (29)$$

The results for the MS RLT tests showed that PD increased with increased w and the moisture sensitivity increased with the increased fines content. The model was calibrated using the test data and its performance was evaluated applying standard statistical procedures. The materials used for this study were three grain size distributions of Skärlunda, Hallinden, Siem 25 and SG1. The model fitted pretty well for the different materials with different w 's. Figure 39 shows the fitted model to the MS RLT test data for two grain size distributions of the Skärlunda UGM having a range of moisture contents. The calibrated parameters of the model and the sensitivity analysis of the parameters to moisture are discussed in the following section which summarizes Paper V.



(a)



(b)

Figure 39. Measured and modelled accumulation of permanent strain for a series of w for the different grain size distributions of the Skärlunda UGMs.

6.5 Paper V: A Model for Predicting PD of UGMs

In this paper, the model proposed in Paper IV was discussed in further detail and was validated with more tests. The sensitivity of its parameters was investigated with respect to moisture, grain size distribution and the degree of compaction. The MS RLT tests were carried out on a several different UGMs with a range of moisture contents. Additionally, one of them was tested with three different grain size distributions, and two others were tested with different degrees of compaction. Figure 40 shows the fitted model to the MS RLT test data for two UGMs having a range of moisture contents. The calibrated parameters of the model for the different materials are presented in Table 8.

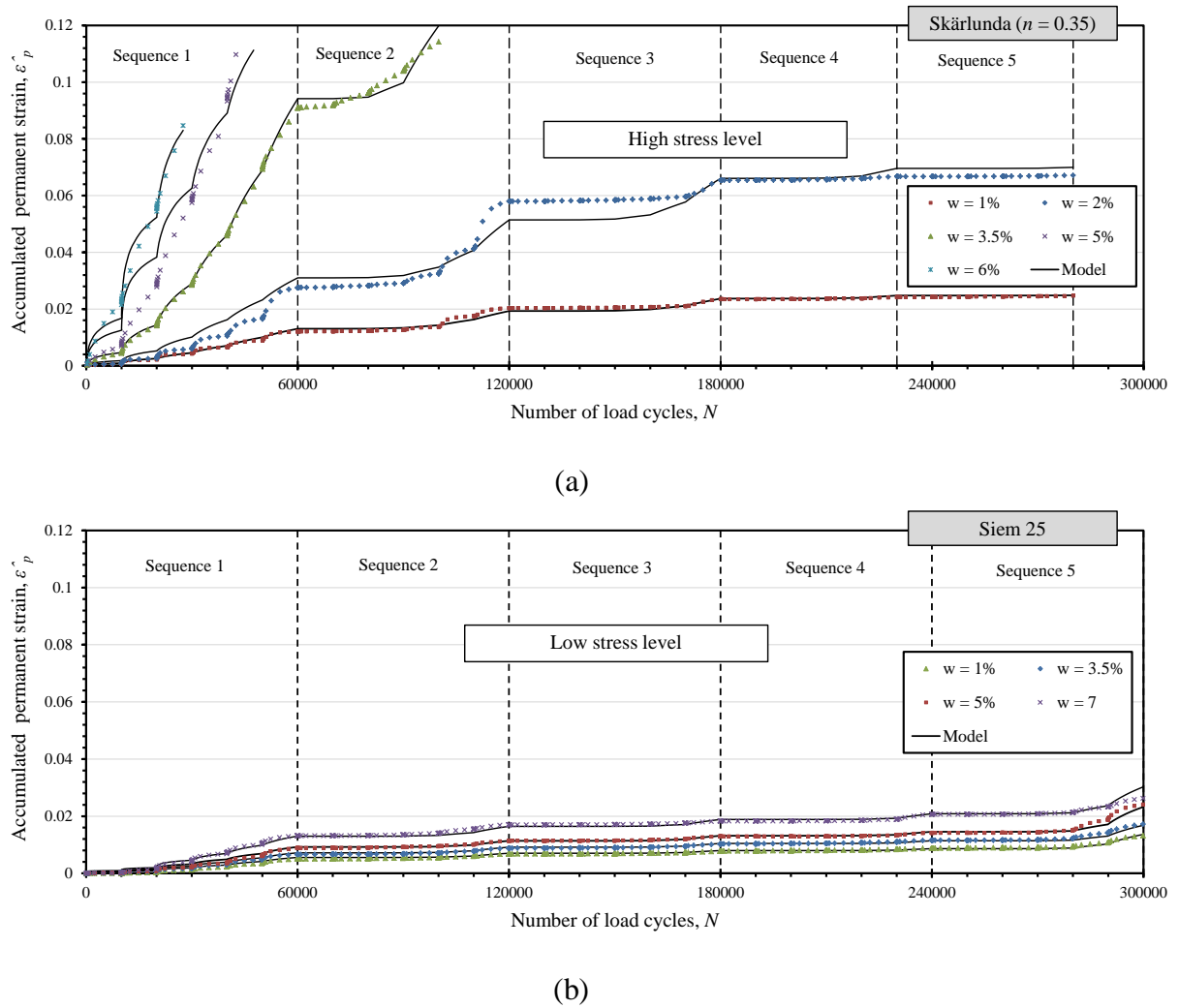


Figure 40. Measured and modelled accumulation of permanent strain for a series of w for different UGMs (during calibration).

Table 8. Calibrated material parameters of the model.

Material	w [% by weight]	Degree of saturation [%]	Dry density [gm/cc]	Degree of compaction [%]	Model parameters ($\alpha = 0.75$)		Quality of fit	
					a	b	R^2	Correct shakedown range predictions [%]
Skärlunda ($n = 0.62$)	1	9.1	2.05	97	0.0049	0.032	0.97	89.3
	3	27.3	2.05	97	0.0054	0.032	0.94	71.4
	5	45.5	2.05	97	0.0066	0.032	0.96	78.6
	7	63.8	2.05	97	0.0081	0.032	0.88	57.1
Skärlunda ($n = 0.45$)	1	12.9	2.19	97	0.0017	0.063	0.99	89.3
	3	38.8	2.19	97	0.0023	0.063	0.99	75.0
	5	64.6	2.19	97	0.0038	0.063	0.99	67.9
	6.5	84.0	2.19	97	0.0058	0.063	0.91	60.7
Skärlunda ($n = 0.35$)	1	11.7	2.15	97	0.0017	0.063	0.99	89.3
	2	23.4	2.15	97	0.0045	0.063	0.94	75.0
	3.5	40.9	2.15	97	0.0123	0.063	0.94	92.9
	5	58.4	2.15	97	0.0185	0.063	0.90	100.0
	6	70.1	2.15	97	0.0253	0.063	0.98	100.0
Hallinden	1	8.6	2.01	97	0.0013	0.065	0.96	93.3
	3.5	30.0	2.01	97	0.0024	0.065	0.95	90.0
	5.5	47.2	2.01	97	0.0029	0.065	0.98	90.0
	6.5	55.7	2.01	97	0.0037	0.065	0.97	93.3
VKB	2	31.6	2.19	99	0.0004	0.134	0.99	76.7
	4.5	71.0	2.19	99	0.0008	0.134	0.91	76.7
	6	94.7	2.19	99	0.0009	0.134	0.73	66.7
SPV	2	26.7	2.23	95	0.0001	0.120	0.71	86.7
	4	53.5	2.23	95	0.0019	0.120	0.98	73.3
	7	78.3	2.16	92	0.0026	0.120	0.50	56.7
	7	85.4	2.20	93.5	0.0024	0.120	0.74	63.3
	7	93.6	2.23	95	0.0023	0.120	0.61	63.3
	7	99.8	2.26	96	0.0023	0.120	0.82	63.3
SG1	3.5	37.8	2.02	95	0.0001	0.119	0.97	89.3
	5.5	59.4	2.02	95	0.0003	0.119	1.00	92.9
	7.5	69.0	1.96	92	0.0014	0.119	0.98	92.9
	7.5	74.6	1.99	93.5	0.0007	0.119	0.93	89.3
	7.5	81.0	2.02	95	0.0004	0.119	0.88	78.6
	7.5	91.0	2.07	97	0.0004	0.119	0.96	100.0
	7.5	98.7	2.09	98.3	0.0003	0.119	0.99	46.4
	8.5	91.8	2.02	95	0.0007	0.119	0.96	78.6
	9.2	99.4	2.02	95	0.0017	0.119	0.85	82.1
Siem 25	1	10.6	2.10	97	0.0004	0.120	0.99	93.3
	3.5	37.2	2.10	97	0.0005	0.120	0.99	93.3
	5	53.1	2.10	97	0.0006	0.120	0.99	93.3
	7	74.4	2.10	97	0.0009	0.120	0.99	96.6

During the calibration of the model, it was observed that $\alpha = 0.75$ yielded pretty good quality of fit for most of the cases. Hence, at this phase of this study, for simplicity, the value of α was fixed to 0.75 for all the cases. Again, for any specific UGM, the value of the parameter b was found to be fairly unaffected by the variation in moisture content. Thus, it was also fixed to a certain value for a specific material. It was also found that a constant value of b for a specific material with different degrees of compaction resulted in quite reasonable quality of fit. Thus, for modelling, only the parameter a stood for the influence of moisture, degree of compaction and grain size distribution on the PD behaviour.

Figure 41 shows the variation of a with moisture for the different UGMs. It shows that a can be assumed as a linear function of w within the range of w used in this study. The best fit lines through these points are also shown in this figure. Hence, the impact of w on a for these materials may be expressed using the following equation:

$$a = c_1(w) + c_2 \quad (30)$$

where c_1 and c_2 are the regression parameters depending on the material. The values of these parameters for the different materials and the corresponding R^2 values are given in Table 9.

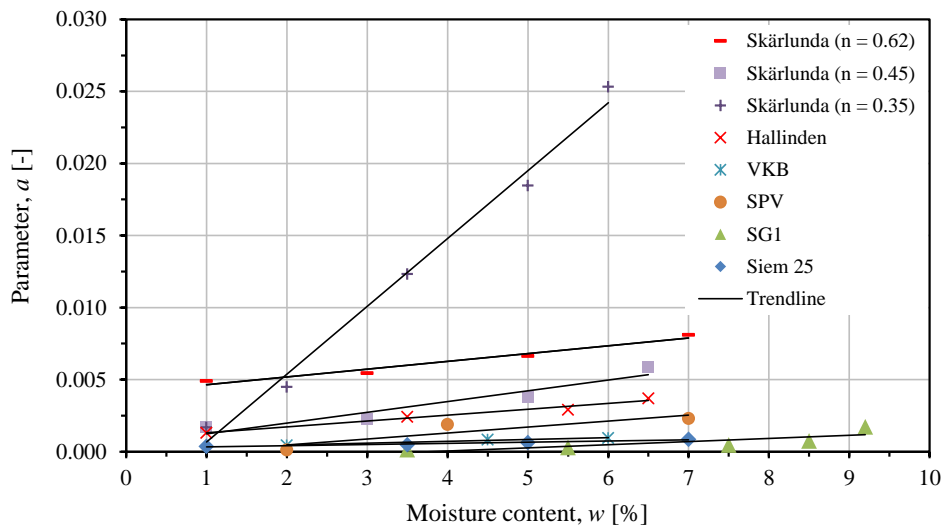


Figure 41. Parameter a as a function of moisture content for the different materials.

Table 9. Parameters of Equation (30).

Material		Skärlanda ($n = 0.62$)	Skärlanda ($n = 0.45$)	Skärlanda ($n = 0.35$)	Hallinden	VKB	SPV	SG1	Siem 25
Parameters	c_1	0.0005	0.0007	0.0047	0.0004	0.0001	0.0004	0.0002	0.00008
	c_2	0.0041	0.0005	-0.004	0.0009	0.0002	-0.0003	0.0008	0.0002
R^2		0.96	0.92	0.99	0.97	0.97	0.86	0.65	0.95

Comparing the three grain size distributions of the Skärlanda aggregates, it was found that the finer gradation was more affected by moisture. Thus the slope of the ‘ a versus w ’ line in Figure 41 is steeper for the finer gradation which is represented by the higher value of c_1 . For VKB, SPV and SG1, the value of c_1 was lower compared to that of Skärlanda UGMs. Although VKB contained a relatively high percentage of fines with a similar gradation as Skärlanda ($n = 0.35$) and SPV, the c_1 value for this material was among the lowest. One possible reason may be that it was tested with a relatively higher degree of compaction (see Table 8). On the other hand, the c_1 value for Siem 25, which contained the least amount of fines, was distinctly lower than that of the other materials, showing less sensitivity to moisture variation. Generally, in this study, it was difficult to compare the sensitivity to moisture with respect to the fines content for different materials. The possible reasons may be that these materials had slightly different grain size distribution curves and there may have been some other material factors and differences in the degree of compaction that influenced the moisture sensitivity. Different packing arrangements of the particles in the different materials may have had some impact (Yideti et al. 2012 and Yideti et al. 2013a). This needs further investigation.

The influence of the degree of compaction was studied by testing two of the materials, SPV and SG1, for a range of degrees of compaction with constant moisture content (different degrees of saturation). Results showed that a lower degree of compaction yielded higher accumulated permanent strain. Thus the value of the parameter a was higher for the lower degree of compaction as shown in Figure 42. Quite similar trends were observed for the two materials. It was possible to fit trend lines with power law functions with pretty acceptable R^2 values, presented in Figure 42. However, it should be emphasized here that only two materials were tested with different degrees of compaction. Furthermore, quite narrow ranges of the degrees of compaction were used because of difficulties in preparing the specimens beyond these ranges (92% to 98.3% of the maximum dry density using the modified Proctor method). Thus the analyses presented here should be verified with further studies.

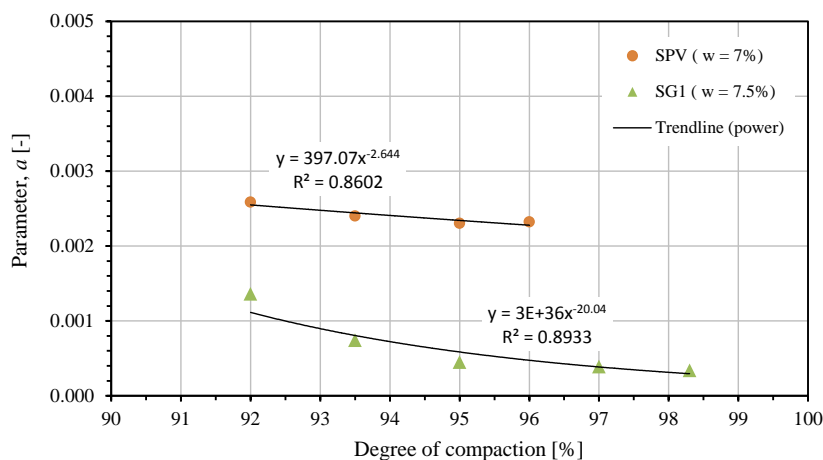
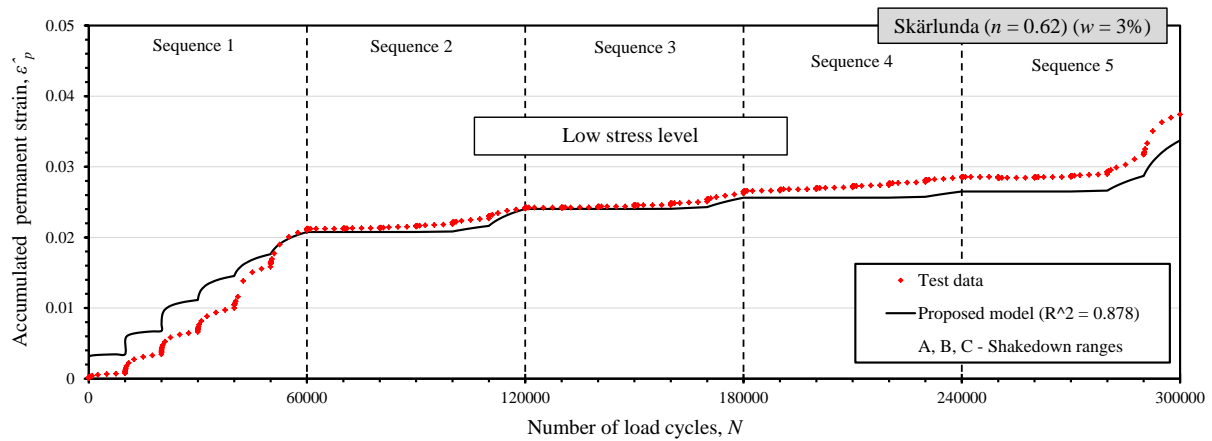
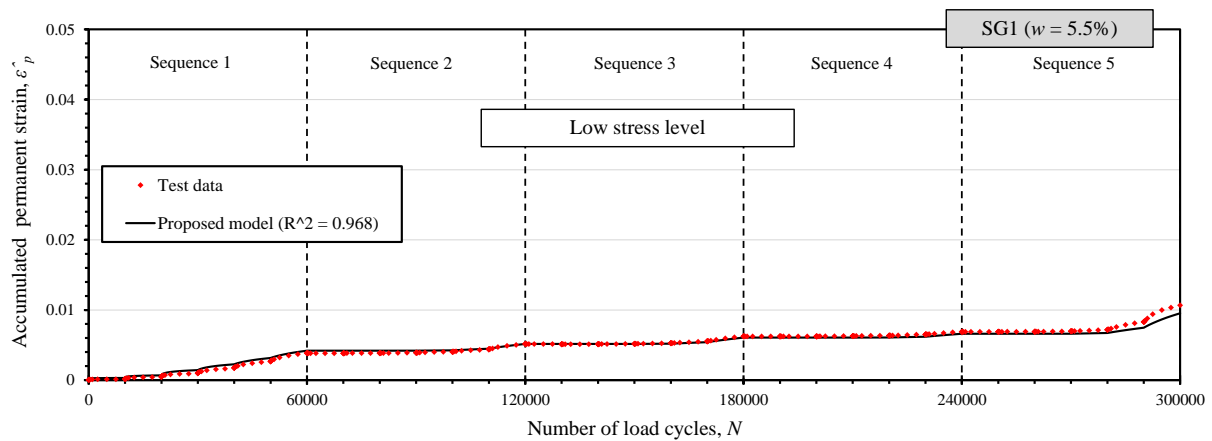


Figure 42. Parameter a as a function of the degree of compaction.

The model was further verified by applying the calibrated model to predict the PD behaviour of the UGMs under a different set of stress levels than that used during the calibration. Since the HSL was used during the calibrations, the accumulations of PD were predicted for the application of LSL on identical specimens. The calculated accumulated permanent strains were then compared to the actual measurements from the MS RLT tests. The quality of predictions was evaluated using the R^2 values. The test data and the predictions by the model are presented in Figure 43. This figure shows that satisfactory predictions of the PD behaviour of the UGMs were obtained using the calibrated model. As can be expected, the quality of fit was not as good as for the calibration tests. One of the possible reasons may be experimental dispersion. The final accumulated strains predicted by the models were, however, pretty close to the observed results. Considering the amount of scatter generally experienced with MS RLT tests on UGMs, these may be considered to be satisfactory.



(a)



(b)

Figure 43. Predicted accumulation of permanent strain using the calibrated models in different stress conditions against the measured values.

7. CONCLUSIONS

The deformation behaviour of UGMs was investigated based on RLT tests. Both the RD and PD properties were studied to improve the characterization and modelling of these properties. The impact of moisture on the deformation behaviour was specifically emphasized here. For the PD characteristics, the use of the MS RLT test was preferred since it enables a more comprehensive study of the material behaviour including the effect of the stress history. Calibrating the models using the MS RLT test makes them applicable for a wide range of stress levels with less effort compared to SS RLT tests. The conclusions that can be drawn from this study are presented below.

7.1 Major findings

In brief, the following were the major findings of this study:

- The resilient stiffness (M_R) of UGMs decreased with increased moisture when the deformation was mostly resilient. However, M_R increased with moisture up to w_{opt} when the RD was accompanied by significant amount of PD due to PC that was aided by the moisture.
- PD always increased with increased moisture.
- The grain size distribution influenced the sensitivity of a UGM to moisture. The materials containing a larger proportion of fine particles were found to be more affected by the moisture variation.
- The parameter k_1 of the $k-\theta$ model decreased with increasing moisture in all cases. On the other hand, the parameter k_2 remained fairly unaffected by moisture when the deformation was mostly resilient but it increased with moisture when a significant amount of PD took place.
- The impact of moisture on M_R was captured well by the MEPDG M_R - moisture model when the deformation was mostly resilient. The modelling approach presented here based on the $k-\theta$ model also worked well in this case. However, when the RD was accompanied by significant amount of PD, the MEPDG model did not work. Although not explored in this study, the modelling approach presented here may work for the latter case if the parameter k_2 is expressed as a function of moisture.
- The time hardening formulation introduced here showed some promising results in predicting the PD behaviour of UGMs in MS RLT tests using the current models. It is a general formulation which is applicable to models similar to those described in section 3.2.1. It is also applicable to similar models for asphalt or any other materials.
- In the comparison of the models in predicting the PD behaviour of UGMs in MS RLT tests, the model by Korkiala-Tanttu performed quite well, followed by the

Gidel et al. model. The model by Tseng and Lytton did not suit as well for the MS RLT tests.

- The model proposed for the PD behaviour of UGMs worked quite well for the MS RLT tests carried out here. The benefit of this model is that it contains relatively fewer material parameters which can be evaluated directly from an MS RLT test.
- Only varying the parameter a of the proposed model yielded quite satisfactory quality of fit for the effect of moisture and degree of compaction. Some trends were observed for the variation of a with moisture and degree of compaction that may be further enhanced to include in the model.

The findings of this study may be useful for the better modelling and prediction of the mechanical behaviour of UGMs in pavement structures which is essential for an ME design approach. This may also aid in selecting a UGM and its grain size distribution considering the strength and drainage requirements for the prevailing traffic and climatic conditions and for enforcing any load restrictions in a particular situation.

7.2 Some limitations

Since this study was based on RLT tests in the laboratory with constant confining pressure, some of the limitations and simplifications of this kind of testing should be applicable here (Araya 2011). Although the RLT test is a widely used method that provides a great deal of information regarding the material behaviour, further work may be necessary to apply some of the findings of this study to all field conditions.

In view of the relatively coarse grain size distributions of the UGMs and the tests carried out under free drainage conditions, the effects of suction and positive pore water pressure were disregarded. Again, the focus of this study was the axial deformation behaviour. Although relatively less significant for this case, the effect of suction and the radial deformation behaviour should be included in future.

For the MS RLT tests, the loading sequences from the European standard (CEN 2004a) were applied in consecutive order. No test was performed by applying the sequences in reversed or random order. It was assumed that applying the sequences in consecutive order would take care of the effect of random loading since the stress paths in the different sequences vary from low to high with some overlapping among the sequences. However, the effect of altering the loading sequences should be considered in future studies.

The parameters of the models used here were optimized to get the best agreement with the measured data based on some initially assumed values. However, there may as well be some other combinations of the values of the parameters that will give a reasonably good fit to the observed data. In this study, no ranges for the parametric values were suggested. For the proposed model, only one parameter was freely optimized while the others were restrained. Although this approach worked reasonably well, more studies need to be carried out regarding the other parameters which may result in even better predictions.

Since RLT tests are time consuming and expensive, only a few regularly used UGMs were tested. Albeit these UGMs are commonly employed in pavement constructions and covered a wide range in terms of grain size distribution and moisture content, the conclusions drawn here should be further investigated with more tests using more different types of materials. Additionally, to account for the variability usually encountered in RLT tests on coarse UGMs, the tests need to be replicated. In this study, some but not all of the tests were replicated. Furthermore, the study on the effect of the degree of compaction was quite limited, using only two materials. This also needs more extensive studies.

7.3 Recommendations for future work

The study on the moisture impact on the RD properties of UGMs showed that accumulated PD from post compaction influences the outcome. Thus with further investigation, this effect should be considered for improved modelling. The approach presented here based on the k - θ model to capture the influence of moisture on M_R showed some promising results. With more tests with different materials, this may be used to develop an alternative model to predict the moisture dependency of M_R , similar to that proposed for the subgrade materials (Rahim and George 2005).

Generally, research regarding the PD behaviour of UGMs is less extensive compared to the RD properties. Regarding the impact of moisture on PD, this is even scarcer. Hence more studies need to be carried out on the PD properties and the influence of moisture. Previous studies on the influence of moisture of the PD behaviour of UGMs are only qualitative. Despite the importance, any well-established model to quantify this effect is still lacking. The study on the sensitivity to moisture of the parameters of the proposed model showed some trends that may be incorporated into the model after further investigation. The effect of the degree of compaction may also be included after more detailed studies. The influence of the grain size distribution and fines content on the PD behaviour also needs further investigation that may be used to develop a model similar to that proposed by Rahim and George (2005) for the M_R of subgrade materials. As discussed in the previous sub-section, further work is also required for the parameters of the proposed model. More work also needs to be carried out to implement the model, which was developed based on RLT tests, to predict the behaviour of UGMs in real pavement structures. Moreover, this model needs to be validated using in situ pavement data, for instance, using data from accelerated pavement tests (APT) such as heavy vehicle simulators (HVS) (Ahmed and Erlingsson, 2013; Saevarsdottir and Erlingsson, 2014).

REFERENCES

- Ahmed, A.W. and Erlingsson, S. (2013). Evaluation of permanent deformation models for unbound granular materials using accelerated pavement tests. *Road Materials and Pavement Design*, 14(1), pp. 178-195, DOI: 10.1080/14680629.2012.755936.
- Andrei, D. (2003). Development of a Predictive Model for the Resilient Modulus of Unbound Materials. *Doctoral thesis*. Arizona State University, USA.
- ARA, Inc. (2004). Guide for the Mechanistic Empirical Design of New and Rehabilitated Pavement Structures. *Final report, NCHRP1-37A*, Transportation Research Board, National Research Council, Washington D.C., USA.
- Araujo, N. and Correia, A.G. (2009). Precision triaxial equipment for the evaluation of the elastic behavior of soils. *Bearing Capacity of Roads, Railways and Airfields – Tutumluer and Al-Qadi (eds.)*, Taylor and Francis Group, London, ISBN 978-0-415-87199-0.
- Araya, A.A. (2011). Characterization of Unbound Granular Materials for Pavements. *Doctoral thesis*. Delft University of Technology, the Netherlands.
- Arnold, G.K. (2004). Rutting of Granular Pavements. *Doctoral thesis*. University of Nottingham, England.
- Arvidsson, H. (2006). Dynamiska treaxialförsök på VTI. Jämförelse mellan VTI-metoder och EN 13286-7 (In Swedish). *VTI notat 21-2006*. VTI (Swedish National Road and Transport Research Institute), Linköping Sweden.
- Burmister, D.M. (1943). The theory of stresses and displacements in layered system and application to the design of airport runways. *Proceedings of the Highway Research Board*, Washington, DC, 23, pp. 126-148.
- Burmister, D.M. (1945). The general theory of stresses and displacements in layered soil system. *Journal of Applied Physics*, 16(2), pp. 89-96, 16(3), pp. 126-127, 16(5), 296-302.
- Cary, C.E. and Zapata, E.C. (2011). Resilient Modulus for Unsaturated Unbound Materials. *Road Materials and Pavement Design*. Vol. 12/13, pp. 615-638.
- CEN-European Committee for Standardization. (2004a). EN 13286-7 Cyclic load triaxial test for unbound mixtures. *European Standard*, Brussels.

- CEN-European Committee for Standardization. (2004b). EN 13286-2 Test methods for the determination of the laboratory reference density and water content – Proctor compaction. *European Standard*, Brussels.
- Chan, F.W.K. (1990). Permanent Deformation Resistance of Granular Layers in Pavements. *Doctoral thesis*. University of Nottingham, England.
- Charlier, R., Hornych, P., Srsen, M., Hermansson, A., Bjarnason, G., Erlingsson, S. and Pavsic, P. (2009). Water influence on bearing capacity and pavement performance: Field observations. *Water in Road Structures*, Chapter 8, Springer Science+Business Media B.V. pp. 23-44.
- Correia A.G. and De Almeida, J.R. (1998). Mechanical behaviour of unbound granular materials for modelling of flexible pavements. *The 5th International Conference on the Bearing Capacity of Roads and Airfields (BCRA)*, July, Trondheim, Norway.
- Dawson, A.R. and Wellner, F. (1999). Plastic Behaviour of Granular Materials. *Final Report, ARC Project 933*, Reference PRG99014, April, 1999. The University of Nottingham.
- Dawson, A.R., Thom, N.H., and Paute, J.L. (1996). Mechanical characteristics of unbound granular materials as a function of condition. *Flexible pavements, Proc. European Symp. Euroflex 1993*, A.G. Correia, ed., Balkema, pp. 35-44.
- Ekblad, J. (2007). Influence of Water on Coarse Granular Road Material Properties. *Doctoral thesis*. Royal Institute of Technology (KTH), Stockholm, Sweden.
- El Abd A., Hornych P., Breyse D., Denis D. (2005). Prediction of permanent deformations of unbound pavement layers. *Proceedings from the 7th International Conference on the Bearing Capacity of Roads and Airfields (BCRA)*, June, Trondheim, Norway.
- El-Basyouny M.M., Witczak M., Kaloush K. (2005). Development of the Permanent Deformation Models for the 2002 Design Guide. *Compendium of Papers of the Annual Meeting of the Transportation Research Board*, January, Washington DC. Transportation Research Board of the National Academies.
- Englund, J. (2011). Analyses of Resilient Behavior of Unbound Materials for the Purpose of Predicting Permanent Deformation Behavior. *Doctoral thesis*. Chalmers University of Technology, Gothenburg, Sweden.
- Erlingsson, S. (2002). 3-D FE Analyses of Test Road Structures – Comparison with Measurements. *Proceedings from the 6th International Conference on the Bearing Capacity of Roads, Railways and Airfields BCRA'02*, Lisbon, Portugal, pp. 145-157.

- Erlingsson, S. (2010). Impact of water on the response and performance of a pavement structure in an accelerated test. *Road Materials and Pavement Design*. Vol. 11/4, pp. 863-880.
- Erlingsson, S. and Ahmed, A.W. (2013). Fast layered elastic response program for the analysis of flexible pavement structures. *Road Materials and Pavement Design*, 14:1, 196-210.
- Erlingsson, S. and Magnúsdóttir, B. (2002). Dynamic Triaxial Testing of Unbound Granular Base Course Materials. *Proceedings from the 6th International Conference on the Bearing Capacity of Roads and Airfields (BCRA)*, Lisbon, Portugal, pp. 989-1000.
- Erlingsson, S., Brencic, M. and Dawson, A. (2009). Water flow theory for saturated and unsaturated Pavement material. *Water in Road Structures*, Chapter 2, Springer Science+Business Media B.V. pp. 23-44.
- Erlingsson, S., Said, S. and McGarvey, T. (2012). Influence of heavy traffic lateral wander on pavement deterioration. *Proceedings of the 4th European Pavement and Asset Management Conference (EPAM4)*, September, Malmö, Sweden.
- Gidel, G., *et al.* (2001). A New Approach for Investigating the Permanent Deformation Behaviour of Unbound Granular Material Using the Repeated Load Triaxial Apparatus. *Bulletin de Liaison des Laboratoires des Ponts et Chaussées*, No. 233, July-August, 2001, 5-21.
- Gujarati, D.N. and Porter, D.C. (2009). Basic Econometrics (5th ed.). McGraw-Hill/Irwin, New York, pp. 73–78. ISBN 978-0-07-337577-9.
- Hicks, R.G. and Monismith, C.L. (1971). Factors Influencing the Resilient Response of Granular Materials. *Highway Research Record 345*, Highway research Board, Washington DC, USA, pp. 15-31.
- Hornych, P. and El Abd, A. (2004). Selection and Evaluation of Models for Prediction of Permanent Deformations of Unbound Granular Materials in Road Pavements. *Competitive and Sustainable Growth (GROWTH) Programme*, SAM-05-DE10.
- Huang, Y.H. (2004). Pavement Analysis and Design (2nd ed.). Prentice Hall, Inc., Englewood Cliffs, NJ, 775 pp.
- Janoo, V.C. (2002). Performance of base/subbase materials under frost action. *Proceedings of the Eleventh International Conference on Cold Regions Engineering*, K. S. Merrill (ed.). Anchorage, AK: American Society of Civil Engineers, pp. 299-310.

- Johnson, R., Freund, J. and Miller, I. (2011). Probability and Statistics for Engineers (8th ed.), *Pearson Education, Inc.* ISBN 13: 978-0-321-69498-0.
- Kolisoja, P. (1997). Resilient Deformation Characteristics of Granular Materials. *Doctoral thesis*. Tampere University of Technology, Tampere, Finland.
- Korkiala-Tanttu, L. (2005). A New Material Model for Permanent Deformations in Pavements. *Proceedings of the 7th International Conference on Bearing Capacity of Roads and Airfields, BCRRA '05*, Trondheim, Norway.
- Laloui, L., Charlier, R., Chazallon, C., Erlingsson, S., Hornych, P., Pavsic, P. and Srsen, M. (2009). Water influence on mechanical behaviour of pavements: Constitutive modelling. *Water in Road Structures*, Chapter 9, Springer Science+Business Media B.V. pp. 193-216.
- Lekarp, F. (1999). Resilient and Permanent Deformation Behavior of Unbound Aggregates under Repeated Loading. *Doctoral thesis*. Royal Institute of Technology (KTH), Stockholm, Sweden.
- Liu, Y., Stolle, D., Guo, P., and Emery, J. (2014). Stress-path dependency of resilient behaviour of granular materials. *International Journal of Pavement Engineering*, 15:7, 614-622, DOI:10.1080/10298436.2013.808340.
- Lytton, R.L., Uzan, J., Fernando, E.G., Roque, R., Hiltunen, D. and Stoffels, S.M. (1993). Development and Validation of Performance Prediction Models and Specifications for Asphalt Binders and Paving Mixes. *The Strategic Highway Research Program Project Report*. No. SHRP-A-357.
- Marsala, A.F., Figoni, A., Pellegrino, A. (2001). Laser Cell for Triaxial Tests on Core Samples: A New Tool for Innovative Mechanical Testing of Rock Materials. *DC Rocks 2001, the 38th U.S. Symposium on Rock Mechanics (USRMS)*, 7-10 July, Washington, D.C., American Rock Mechanics Association, ARMA-01-1267.
- Morgan, J.R. (1966). The response of granular materials to repeated loading. *Proceedings of the Third Conference, ARRB*, 1178-1192.
- Qiao, Y., Dawson, A., Huvstig, A. and Korkiala-Tanttu, L. (2014). Calculating rutting of some thin flexible pavements from repeated load triaxial test data. *International Journal of Pavement Engineering*, DOI: 10.1080/10298436.2014.943127.
- Rahim, A.M. and George, K.P. (2005). Models to estimate subgrade resilient modulus for pavement design. *International Journal of Pavement Engineering*, 6:2, 89-96, DOI: 10.1080/10298430500131973.

- Richter, C.A. and Schwartz C.W. (2003). Modeling stress- and moisture-induced variations in pavement layer moduli. *Compendium of Papers of the Annual Meeting of the Transportation Research Board of the National Academies*, January, Washington DC, USA.
- Saevarsdottir T. and Erlingsson S. (2014). Modelling of responses and rutting profile of a flexible pavement structure in a heavy vehicle simulator test. *Road Materials and Pavement Design*, DOI: 10.1080/14680629.2014.939698.
- Saevarsdottir, T. and Erlingsson, S. (2013). Water impact on the behaviour of flexible pavement structures in an accelerated test. *Road Materials and Pavement Design*, DOI: 10.1080/14680629.2013.779308.
- Salour, F. and Erlingsson, S. (2013). Investigation of a pavement structural behaviour during spring thaw using falling weight deflectometer. *Road Materials and Pavement Design*, 14:1, 141-158.
- Schwartz, C.W. (2002). Effect of Stress-Dependent Base Layer on the Superposition of Flexible Pavement Solutions. *The International Journal of Geomechanics*, Volume 2, Number 3, pp. 331–352.
- Seed, H.B., Chan, C.K. and Lee, C.E. (1962). Resilient characteristics of subgrade soils and their relations to fatigue in asphalt pavements. *Proceedings of International Conference on Structural Design of Asphalt Pavements*. Ann Arbor, USA. Vol. 1, pp. 611-636.
- Tao, M., *et al.* (2010). Application of shakedown theory in characterizing traditional and recycled pavement base materials. *Journal of Transportation Engineering*, American Society of Civil Engineers (ASCE), No. 136/3, 214-222.
- Tholen, O. (1980). Falling weight Deflectometer – a device for bearing capacity measurements: Properties and performance. *Degree project*. Department of Highway Engineering, Royal Institute of Technology (KTH), Stockholm, Sweden.
- Thom, N.H. and Brown, S.F. (1987). Effect of moisture on the structural performance of a crushed-limestone road base. *Transport Research Record 1121*, Transportation Research Board, Washington DC, USA, pp. 50-56.
- Tseng, K.H. and Lytton, R.L. (1989). Prediction of permanent deformation in flexible pavement materials. *Implication of Aggregates in Design, Construction, and Performance of Flexible Pavements*, ASTM STP 1016, H. G. Schrauders, and C. R. Marek, eds. American Society for Testing and Materials, Philadelphia, pp. 154-172.
- Uzan, J. (1985). Characterization of granular material. *Transportation Research Record 1022*, Transportation Research Board, Washington DC, USA, pp. 52-59.

- Uzan, J. (1999). Permanent Deformation of a Granular Base Material. *Compendium of Papers of the 78th Annual Meeting of the Transportation Research Board of the National Academies*, January, Washington DC, USA.
- Uzan, J. (2004). Permanent deformation in flexible pavements. *Journal of Transportation Engineering*, American Society of Civil Engineers (ASCE), No. 130(1), pp. 6-13.
- Uzan, J., Witczak, M.W., Scullion, T. and Lytton, R.L. (1992). Development and validation of realistic pavement response models. *Proceedings of the 7th International Conference on Asphalt Pavements*. Nottingham. Vol. 1, pp. 334-350.
- Werkmeister, S. (2003). Permanent Deformation Behavior of Unbound Granular Materials. *Doctoral thesis*. Dresden University of Technology, Dresden, Germany.
- Werkmeister, S. (2006). Shakedown analysis of unbound granular materials using accelerated pavement test results from New Zealand's CAPTIF Facility. *Pavement Mechanics and Performance*, American Society of Civil Engineers (ASCE), No. 154, pp. 220–228.
- Werkmeister, S., Dawson, A.R. and Wellner, F. (2001). Permanent deformation behavior of granular materials and the shakedown concept. *Transport Research Record 1757*, Transportation Research Board, Washington DC, USA, Paper No. 01-0152, pp. 75-81.
- Werkmeister, S., Dawson, A.R. and Wellner, F. (2004). Pavement design model for unbound granular materials. *Journal of Transportation Engineering*, American Society of Civil Engineers (ASCE), No. 130(5), pp. 665–674.
- Wright, P.H. (1996). Highway Engineering (6th ed.). *John Wiley and Sons, Inc.*, ISBN 0-471-00315-8.
- Wu, R., and Harvey, J.T. (2008). Evaluation of the Effect of Wander on Rutting Performance in HVS tests. *Proceedings of the 3rd International Conference on Accelerated Pavement Testing*, October, Madrid, Spain.
- Yideti, T.F., Birgisson, B. and Jelagin, D. (2013a). Influence of aggregate packing structure on California bearing ratio values of unbound granular materials. *Road Materials and Pavement Design*, 15(1), pp. 102-113, DOI:10.1080/14680629.2013.863160.
- Yideti, T.F., Birgisson, B., Jelagin, D. and Guarin, A. (2012). Packing theory-based framework to evaluate permanent deformation of unbound granular materials. *International Journal of Pavement Engineering*, 14(3), pp. 309-320, DOI:10.1080/10298436.2012.736620.

- Yideti, T.F., Birgisson, B., Jelagin, D., and Guarin, A. (2013b). Packing theory-based framework for evaluating resilient modulus of unbound granular materials. *International Journal of Pavement Engineering*, 13:5, 689-697, DOI:10.1080/10298436.2013.857772.

APPENDED PAPERS

